Diffusion Tensor Imaging connectivity analysis: detecting structural alterations and their underlying substrates for Optic Ataxia in correlations with "How" stream Visual Pathways

Ganesh Elumalai, Panchanan Maiti, Geethanjali Vinodhanand, Valencia Lasandra Camoya Brown, Nitya Akarsha Surya Venkata Ghanta, Venkata Hari Krishna Kurra
[1]Team NeurON – Brain Research Laboratory, Saginaw Valley State University, MI, USA.

Abstract

Optic ataxia is a neurological condition that shows clinical manifestations of disturbances in visual guided hand movements on reaching for a target object. Previous studies failed to provide substantial evidences for the neural structural pathway damaged by this condition. Therefore, this study was aimed to identify the neural structural connectivity between "Visual cortex with Superior Parietal Lobule" and to correlate its functional importance, using "Diffusion Imaging fiber Tractography. The fibers were traced, and we confirmed its extension from "Visual cortex (Brodmann's Areas 18 and 19) to Superior Parietal Lobule (Brodmann's Area 7)". This new observation gives an insight to understand the structural existence and functional correlations between "Visual cortex with Superior Parietal Lobule" which is involved in targeting the grasping hand movements towards a visually perceived object, called visuo-motor coordination pathway or "how" stream pathways in visual perception. The observational analysis used thirty-two healthy adults, ultra-high b-value, diffusion MRI datasets from an Open access research platform. The datasets range between 20–49 years, in both sexes, with mean age of 31.1 years. The confirmatory observational analysis process includes, datasets acquisition, pre-processing, processing, reconstruction, fiber tractography and analysis using software tools. All the datasets confirmed that the fiber structural extension between, Visual cortex to superior parietal lobe in both the sexes may be responsible for the visual spatial recognition of objects. These new fiber connectivity evidences justify the structural relevance of visual spatial recognition impairments, such as optic ataxia.

Keywords: DTI Tractography, "Dorsal" stream visual pathway, Superior Parietal Lobule, "Where" stream Visual pathways, "How" stream visual pathway.

1. Introduction

Many past references have proposed that the Dorsal stream visual pathway contributes to the visual-spatial recognition of an object hence, the orientation of an object in the space is achieved by the dorsal stream visual pathway. Mishkin and Ungerleider had found two streams visual pathway where the dorsal and the ventral streams contribute to locate and perceive different kinds of objects that are presented to a person, therefore, dorsal stream visual pathway is a multi-synaptic cortico-cortical pathway [1] that enables a person to guide the actions visually towards an object. Dorsal stream is an occipitoparietal pathway where there is white matter connection from the primary visual cortex (Brodmann area 17,18,19) [2] to the superior parietal lobe (Brodmann area 7). Rizzolatti and Matelli have stated that the dorsal stream visual pathway is anatomically formed by two different functional systems namely the dorso-dorsal and the ventro-dorsal streams [3]. Both the functions of the dorso-dorsal and ventro-dorsal streams are to link actions with the visual perception [3]. To grasp and to have a grip of an object is definite with the dorsal stream (occipitoparietal stream) as proposed by Culham and Stacey [4]. Milner and Goodale stated that the information provided by the dorsal stream is viewer - centered information where the object is viewer - centered, and the information is grasped [5]. Polanen and Davare mentioned that the ventral stream sends information about the object's identity to the dorsal stream so that the dorsal stream can help to locate the object, hence we conclude by saying that firstly, the "WHAT" pathway gets activated and then the "WHERE" pathway [6], [7]. Some references mention that there is a direct white matter connection between the dorsal and ventral stream. Bilateral damage to the occipitoparietal connection can lead to optic ataxia. As our previous references haven't mentioned any structural connection, we Team NeurON have observed a new finding that there is an existence of a neural structural connection between the primary visual cortex and the superior parietal lobe. Optic ataxia is a high order neurological deficit where the person cannot locate objects that are spatially oriented, hence, we are stating that due to the damage to the interconnection between the visual cortex and superior parietal lobe, there might be deficits in normal spatial orientation of objects. Scientists have given proof that the optic ataxia can lead to a damage to "HOW" pathway. In the case of Alzheimer's, we found that patients present with optic ataxia which is one of the most important symptoms found in these

patients of recent. Patients of Alzheimer's with optic ataxia do not have coordination in object-oriented hand movements nor in grasping of objects [8].

2. MATERIALS AND METHODS

The present study design used the open access, ultra-high b-value, diffusion imaging datasets from Massachusetts General Hospital – US Consortium Human Connectome Project (MGH-USC HCP) acquired from Thirty-five healthy adults' participants (16 Males and 16 Females, between the 20–59 years). The imaging data is available to those who register and agree to the Open Access Data Use Terms.

2.1 Participants

Data was acquired from thirty- two healthy adults between the ages of 20 to 59. The participants gave written consent, and the procedures were carried out in accordance with the Institutional review board (MGH/HST) approval and procedures. All participants who participated in the MGH-USC Adult Diffusion Dataset were scanned on the 3T CONNECTOM MRI scanner (see (Setsompop et al., 2013) for an overview) housed at the Athinoula A. Martinos Center for Biomedical Imaging at MGH. A custom-made 64-channel phased array head coil was used for signal reception (Keil et al., 2013).

Thirty-two healthy adults participated in this study (16 Females, 16 males, 20–59 years old; mean age = 31.1 years old). All participants gave written informed consent, and the experiments were carried out with approval from the institutional review board of Partners Healthcare. Participants' gender and age are available in the data sharing repository, Due to the limited sample size there are some ages for which we had only one participant. Given de-identification considerations, age information is provided in 5-year age bins.

2.2 Data Acquisition

The data was collected on the customized Siemens 3T Connectome scanner, which is a modified 3T Skyra system (MAGNETOM Skyra Siemens Healthcare), housed at the MGH/HST Athinoula A. Martinos Center for Biomedical Imaging. A 64-channel, tight-fitting brain array coil was used for data acquisition. dMRI data were acquired using a mono-polar Stejskal-Tanner pulsed gradient spin- echo planar imaging (EPI) sequence with Parallel imaging using Generalized Auto calibrating

Partially Parallel Acquisition (GRAPPA). The Fast Low-angle Excitation Echo-planar Technique (FLEET) (Polimeni et al., 2015) was used for Auto-Calibration Signal (ACS) acquisitions to reduce motion sensitivity of the training data and improve stability and SNR of the GRAPPA reconstructions. The Simultaneous Multi-Slice (SMS; multi-band) technique (Feinberg et al., 2010; Feinberg and Setsompop, 2013; Setsompop et al., 2012a; Setsompop et al., 2012b) has been shown to increase the time efficiency of diffusion imaging and was considered for this protocol, however at the point in the project timeline when data acquisition was to begin, the SMS method was not implemented in the EPI sequence featuring FLEET-ACS for GRAPPA. Because of the key benefits of in-plane acceleration for improved EPI data quality, such as lower effective echo spacing and hence mitigated EPI distortions and blurring, and also because of the longer image reconstruction times associated with SMS-EPI data, here data acquisition was performed without the use of SMS in favor of in-plane acceleration using FLEET-ACS and GRAPPA. (Acquisition of subsequent datasets including the Life Span dataset utilized a more newly implemented sequence combining SMS-EPI with FLEET-ACS and GRAPPA, see below.)

In each subject, dMRI data was collected with 4 different b-values (i.e., 4 shells): 1000 s/mm2 (64 directions), 3000 s/mm2 (64 directions), 5000 s/mm2 (128 directions), and 10000 s/mm2 (256 directions). Different b-values were achieved by varying the diffusion gradient amplitudes, while the gradient pulse duration (δ) and diffusion time (Δ) were held constant. These b-values were chosen to provide some overlap with the HCP data from WU-Minn consortium, while at the same time push to the limit of diffusion weighting within the constraints of SNR and acquisition time. On determining the number of directions in each shell, in general, data with higher b-value were acquired with more DW directions to capture the increased ratio of high angular frequency components in the MR signal, and to compensate for the SNR loss due to increased diffusion weighting. Also, the number of directions in each shell were selected to meet the typical requirements of popular single shell and multi-shell analysis methods (e.g. q-ball imaging (Descoteaux et al., 2007; Tuch, 2004; Tuch et al., 2002; Tuch et al., 2003), spherical deconvolution (Anderson, 2005; Dell'Acqua et al., 2007; Tournier et al., 2004), ball and stick model (Behrens et al., 2007; Jbabdi et al., 2012), multi-shell q-ball imaging (Aganj et al., 2010; Yeh et al., 2010), diffusion

propagator imaging (Descoteaux et al., 2009, 2011), etc.), and to keep the total acquisition time feasible in healthy control subjects.

The diffusion sensitizing direction sets were specifically designed so that the 64-direction set is a subset of the 128-direction set, which is again a subset of the 256-direction set. The initial 64 directions were calculated with the electro-static repulsion method (Caruyer et al., 2013; Jones et al., 1999). With these 64 directions fixed, another 64 directions were added as unknowns, and an optimized 128- direction set was calculated by adjusting the added 64 directions using electrostatic repulsion optimization. With these 128 directions fixed, the 256-direction set was generated using the same method. As such, all 4 shells share the same 64 directions; the b=5000 s/mm2 shell and the b=10000 s/mm2 shell share the same 128 directions.

During data acquisition, the diffusion sensitizing directions with approximately opposite polarities were played in pairs to counter-balance the eddy current effects induced by switching the diffusion weighting gradient on and off. Each run started with acquiring a non- DW image (b=0), and one non-DW image was collected every 13 DW images thereafter. Therefore 552 image volumes were collected in total, including 512 DW and 40 non-DW volumes for each subject.

2.3 DTI Data Pre-processing and Quality Control

The MGH-USC HCP team completed their basic imaging data preprocessing, with software tools in Free surfer and FSL, which includes (i) Gradient nonlinearity correction, (ii) Motion correction, (iii) Eddy current correction, (iv) b-vectors.

All DTI data were corrected for gradient nonlinearity distortions offline (Glasser et al., 2013; Jovicich et al., 2006). Diffusion data was further corrected for head motion and eddy current artifacts. Specifically, the b=0 images interspersed throughout the diffusion scans were used to estimate bulk head movements with respect to the initial time point (the first b=0 image), where rigid transformation was calculated using the boundary-based registration tool in the Free Surfer package V5.3.0 (Greve and Fischl, 2009). For each b=0 image, this transformation was then applied to itself and the following 13 diffusion weighted images to correct for head motion. Data of all 4 b-

values were concatenated (552 image volumes in total) and passed into the EDDY tool (Andersson et al., 2012) for eddy current distortion correction and residual head motion estimates. The rigid rotational components of the motion estimates were then used to adjust the diffusion gradient table for later data reconstruction purposes.

Both unprocessed and minimally pre-processed data are available for download in compressed NIfTI format. The measured gradient field nonlinearity coefficients are protected by Siemens as proprietary information. Because the gradient nonlinearity correction cannot be performed without this information, the unprocessed data provided have already been corrected for gradient nonlinearity distortions with no other pre-processing performed.

All the anatomical scans (T1w and T2w) were free from gross brain abnormalities as determined by an MGH trained physician. All MRI data (T1w, T2w and DW) went through the process of quality assessment by an MGH faculty member, MGH postdoctoral researcher and an MGH research assistant, all trained in neuroimaging in MGH. More specifically, each dataset was assessed by two raters, who viewed both the unprocessed and minimally pre-processed data volume by volume, and rated in terms of head movements, facial and ear mask coverage (to make sure that brain tissue was not masked off), and eddy current correction results. Finally, a comprehensive grade was given to determine whether a dataset had passed quality control.

2.4 SUMMARY OF DATASETS:

This data set was originally from the MGH-USC HCP team has released diffusion imaging and structural imaging data acquired from 32 young adults using the customized MGH Siemens 3T Connectome scanner, which has 300 mT/m maximum gradient strength for diffusion imaging. A multishell diffusion scheme was used, and the b-values were 1000, 3000, 5000 and 9950 s/mm2. The number of diffusion sampling directions were 64, 64, 128, and 256. The in-plane resolution was 1.5 mm. The slice thickness was 1.5 mm.

2.5 FIBER TRACTOGRAPHY:

Fiber tractography is a very elegant method, which can used to delineate individual fiber tracts from diffusion images. The main process of study, uses the "DSI-Studio" software tools for i. Complete preprocessing, ii. Fiber tracking and iii. Analysis.

The imaging data processing helps to convert the pre-processed raw data to .src file format, which will be suitable for the further reconstruction process. The reconstruction of .src files achieved through a software tool. It converts the .src imaging data to .fib file format. Only the .fib files are compatible for fiber tracking. To delineate individual fiber tracts from reconstructed diffusion images (.fib file), using a DSI studio software tools.

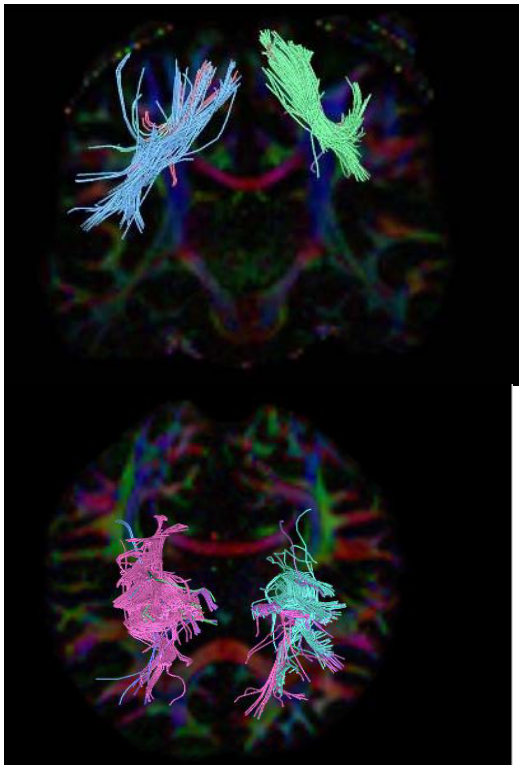

(Fig 3) Coronal Section Male Bi – hemispheric

(Fig 4) Axial Section Female Bi – hemispheric

3.RESULTS

A) Number of tracts

The purpose of our study is deemed to find the neural structures extending between two

cortices, connecting them from one end to another end. Fiber tracking uses diffusion tensor to track the fibers along the whole length starting from the seed to end region. The resolution of finding number of tracts helps us to correlate the actual function of dorsal stream visual pathway;

a) Male Right and Left Side

b) Female Right and Left side

c) Right side Male and Female

d) Left side Male and Female

a) Number of Tracts in Male Subjects Right and Left

We selected sixteen healthy adults' male participants for our study having a mean age of 30.4 years.

Right Side:

The number of tracts were analyzed in 16 male subjects by tracing the neural structural connectivity between the primary visual cortex to Inferior Temporal Lobe, we found that the male subject with the mean age of 32.5 years has highest number of tracts.

Left Side:

The number of tracts were analyzed in 16 male subjects by tracing the neural structural connectivity between the primary visual cortex to Inferior Temporal Lobe, we found that the male subject (1007) with the mean age of 52 has the least number of tracts, (Table 1).

TABLE 1 NUMBER OF TRACTS IN MALE RIGHT AND LEFT*

Subject	SIDE	Number of tracts Male	SIDE	Number of tracts Male
1006	R	4	L	2
1007	R	8	L	194
1008	R	8	L	4
1009	R	45	L	20
1011	R	2	L	8
1013	R	25	L	11
1014	R	42	L	53

1015	R	8	L	20
1016	R	10	L	38
1022	R	6	L	11
1025	R	8	L	1
1027	R	16	L	18
1028	R	111	L	19
1029	R	7	L	29
1030	R	2	L	31
1031	R	26	L	11

The *p*-value is .513463 *The results were statistically ***not significant*** $p < .10$

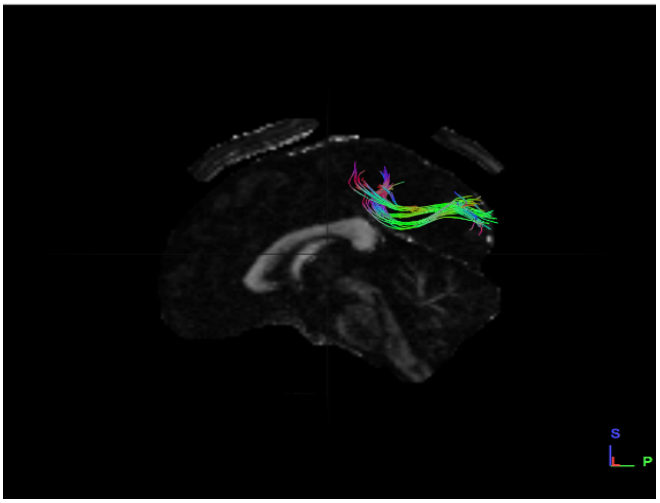

(Fig 1) Sagittal Section Male Left Side Dataset

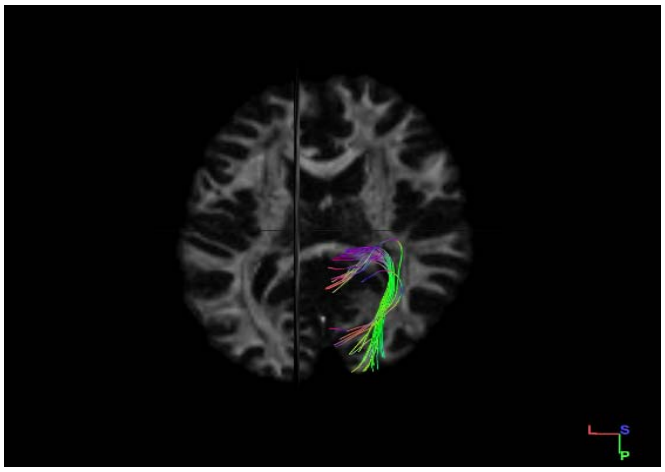

(Fig 2) Axial Section Male Right Side Dataset

Graphical Representation

(Grap-1) Number of tracts in male subjects on both left and right sides.

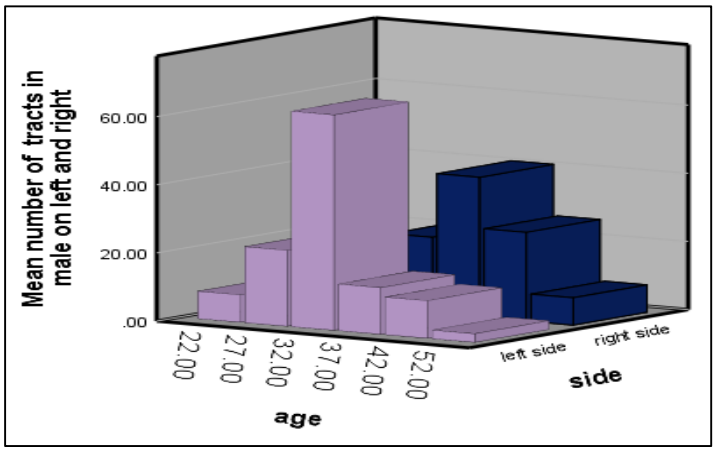

We found that on average, the left side has a greater number of tracts than on right side in male subjects.

b) Number of Tracts in Female Subjects Right and Left

We selected sixteen healthy adult female participants for our study, having a mean age of 30.4 years.

Right Side:

The number of tracts were analyzed in 16 female subjects by tracing the neural structural connectivity between the primary visual cortex to Inferior Temporal Lobe, we found the male subject (1033) with the mean age of 42 years having highest number of tracts.

Left Side:

The number of tracts were analyzed in 16 female subjects by tracing the neural structural connectivity between the primary visual cortex to Inferior Temporal Lobe, we found the female subject (1001) with the mean age of 22 having least number of tracts, (Table 2).

TABLE 2 NUMBER OF TRACTS IN FEMALE RIGHT AND LEFT*

Subject	SIDE	Number of tracts	SIDE	Number of tracts
1001	R	17	L	1
1002	R	69	L	50

1003	R	66	L	316
1004	R	4	L	35
1005	R	55	L	14
1010	R	70	L	6
1012	R	17	L	2
1017	R	16	L	67
1019	R	4	L	39
1021	R	13	L	32
1023	R	4	L	79
1024	R	7	L	6
1026	R	7	L	62
1032	R	14	L	14
1033	R	405	L	10
1035	R	9	L	9

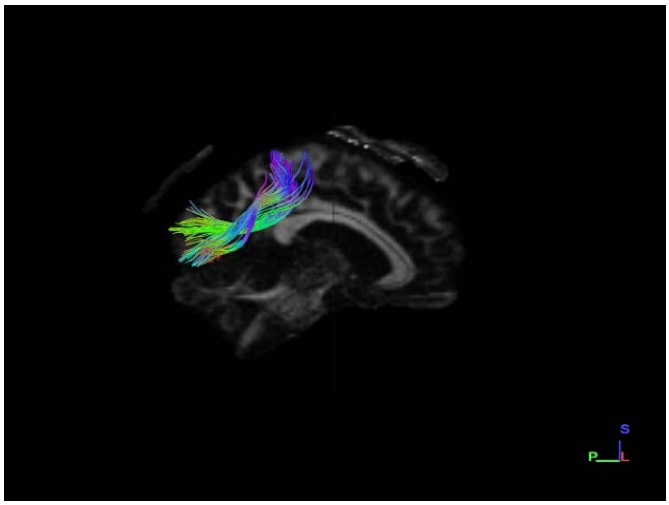

(Fig 3) Sagittal Section Female Right Side Dataset

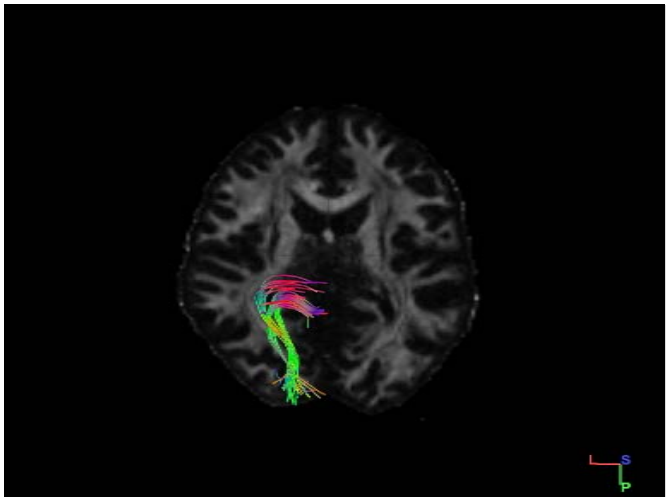

(Fig 4) Axial Section Female Left Side Dataset

Graphical Representation

(Grap-2) Number of tracts in female subjects on both left and right sides.

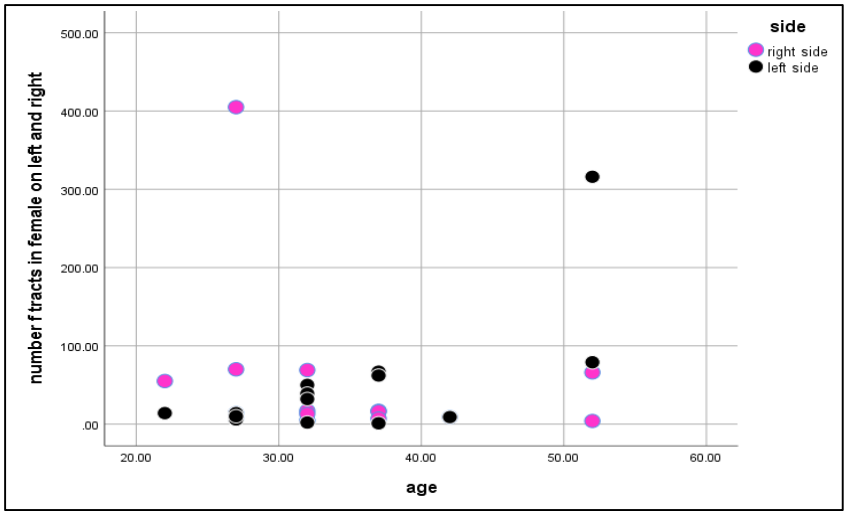

We found the right side having greater number of tracts than left side in female subjects.

TABLE 3 NUMBER OF TRACTS IN MALE AND FEMALE RIGHT *

Female Datasets	Number of tracts Right	Male Datasets	Number of tracts Right
1001	17	1006	4
1002	69	1007	8

1003	66	1008	8
1004	4	1009	45
1005	55	1011	2
1010	70	1013	25
1012	17	1014	42
1017	16	1015	8
1019	4	1016	10
1021	13	1022	6
1023	4	1025	8
1024	7	1027	16
1026	7	1028	111
1032	14	1029	7
1033	405	1030	2
1035	9	1031	26

The p-value is .280034. The result was statistically *not* significant at $p < .10$

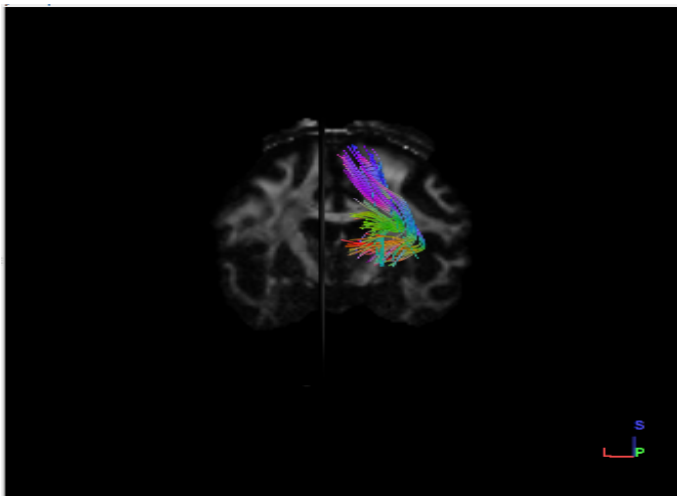

(Fig 4) Coronal section female right side dataset

(Figure 5) Coronal section male right side dataset

We found that female subjects have greater number of fibers on the right side than in male subjects.

TABLE 4 NUMBER OF TRACTS IN MALE AND FEMALE LEFT *

Female datasets	Number of tracts Left	Male Datasets	Number of tracts Left
1001	1	1006	2
1002	50	1007	194
1003	316	1008	4
1004	35	1009	20
1005	14	1011	8
1010	6	1013	11
1012	2	1014	53
1017	67	1015	20
1019	39	1016	38
1021	32	1022	11
1023	79	1025	1
1024	6	1027	18
1026	62	1028	19
1032	14	1029	29
1033	10	1030	31

1035	9	1031	11

The *p*-value is .4507. *The result was statistically *not* significant at $p < .10$.

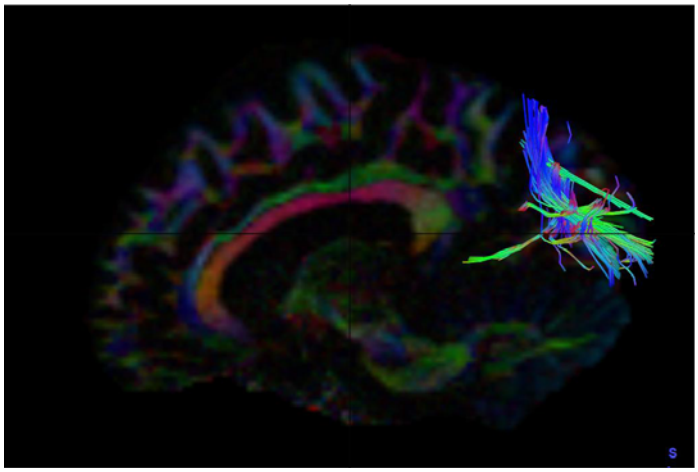

(Fig 6) Sagittal section female left side dataset

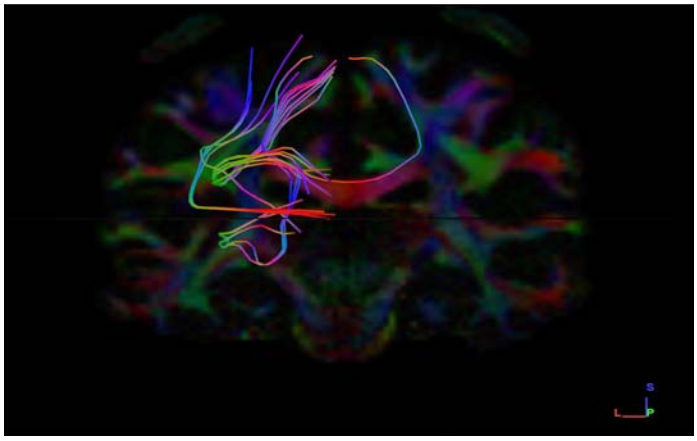

(Fig 7) Coronal section male left side dataset

Graphical Representation

(Grap-3) Number of tracts in both male and female subjects left side.

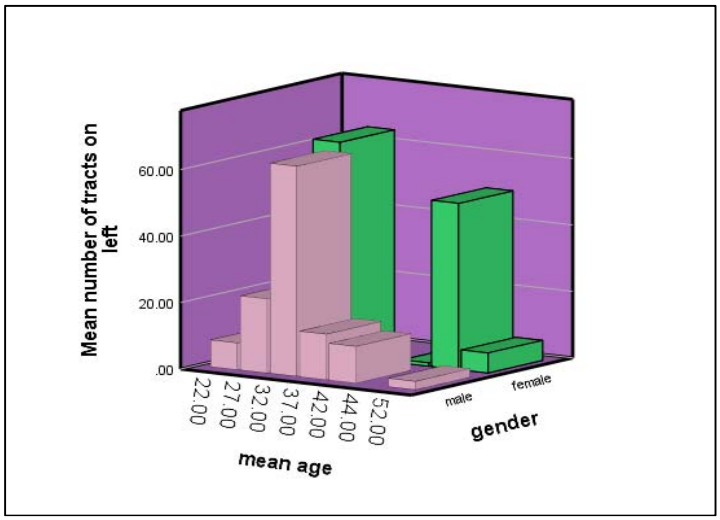

We found that female subjects have greater number of fibers on left side than in male subjects.

B) Volume of tracts

Tract volume is the total volume occupied by fibres collectively. Total volume is otherwise called the total number of voxels that were assigned as containing neural fibers. The comparison of volume of Fibers is mostly done between the seed and the end region under four parameters;

a) Male Right and Left Side

b) Female Right and Left side

c) Right side Male and Female

d) Left side Male and Female

a) Volume of Tracts in Males, both Right and Left Side

We selected sixteen healthy adult male participants for our study having a mean age of 30.4 years.

Right Side:

The Volume of tracts were analyzed in 16 male subjects by tracing the neural structural connectivity between the primary visual cortex to Inferior Temporal Lobe, we found that the male subject (1028) with the mean age of 32.5 years having highest volume of tracts.

Left Side:

The number of tracts were analyzed in 16 male subjects by tracing the neural structural connectivity between the primary visual cortex to Inferior Temporal Lobe, we found that the male subject (1025) with the mean age of 37 having least volume of tracts, (Table 5).

TABLE 5 VOLUME OF TRACTS IN MALE RIGHT AND LEFT**

Subjects	SIDE	Volume of Tracts (mm ^)	SIDE	Volume of tracts (mm ^ 3)
1006	R	712.1251	L	13.0699
1007	R	1191.38	L	11.1297
1008	R	2203.8	L	29.3419
1009	R	5001.75	L	29.8612
1011	R	540	L	3.09596
1013	R	2683.13	L	12.7566
1014	R	3763.13	L	8.55175
1015	R	1748.25	L	9.15248
1016	R	1819.12	L	13.6044
1022	R	894.375	L	18.4829
1025	R	1545.75	L	0
1027	R	2703.38	L	11.6117
1028	R	7661.25	L	5.31415
1029	R	1144.12	L	8.86962
1030	R	492.75	L	8.30297
1031	R	2791.12	L	14.6043

The p-value is .000034. **The result was statistically significant at $p < .1$

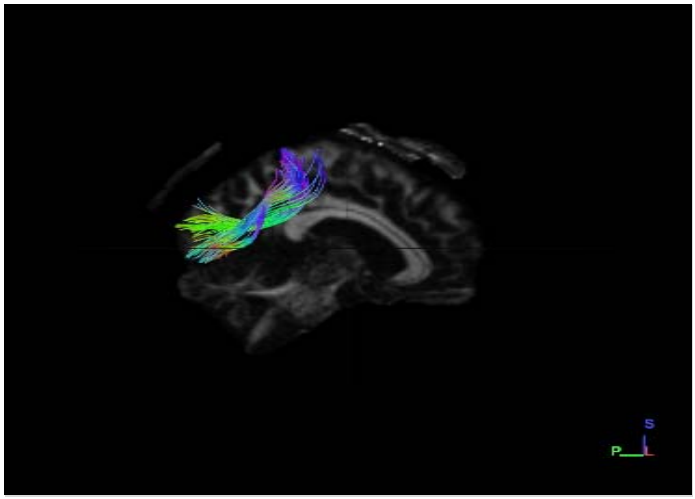

(Fig 8) Sagittal section male right side dataset

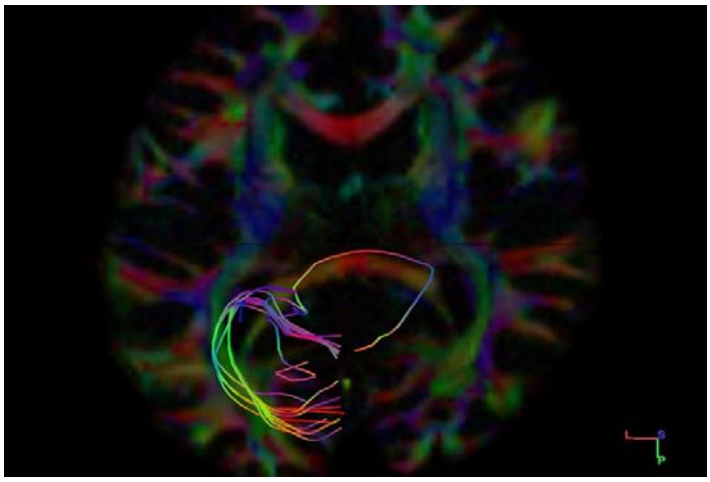

(Fig 9) Axial section male left side dataset

Graphical Representation

(Grap-4) Tract volume in male subjects on left and right sides.

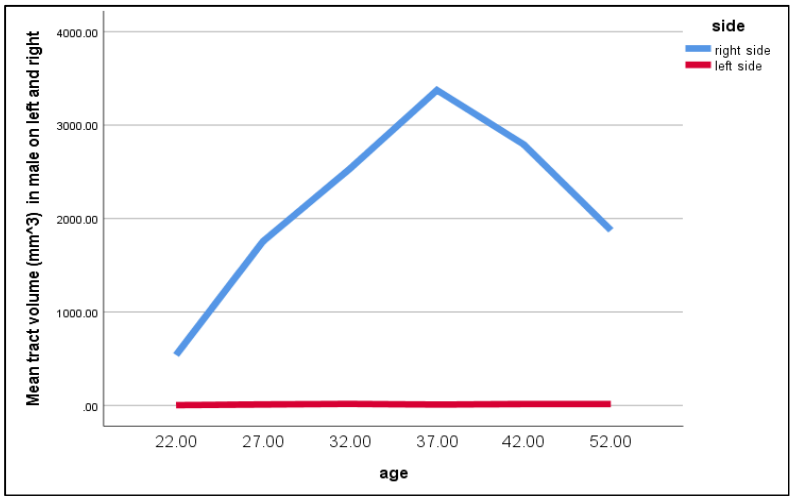

We found that on average, the right side is having greater volume of tracts than on left side in male subjects.

b) Volume of Tracts in Females on both Right and Left Side

We selected sixteen healthy adult female participants for our study, having a mean age of 30.4 years.

Right Side:

The Volume of tracts were analyzed in 16 female subjects by tracing the neural structural connectivity between the primary visual cortex to Inferior Temporal Lobe, we found that the female subject (1010) with the mean age of 27 years having highest number of tracts.

Left Side:

The volume of tracts was analyzed in 16 female subjects by tracing the neural structural connectivity between the primary visual cortex to Inferior Temporal Lobe, we found that the female subject (1001) with the mean age of 41.4 having least volume of tracts, (Table-6).

TABLE 6 VOLUME OF TRACTS IN FEMALE RIGHT AND LEFT**

Subjects	SIDE	Volume of Tracts(mm^)	SIDE	Volume of tracts(mm^3)
1001	R	2072.25	L	0
1002	R	4556.25	L	59.3764

1003	R	4910.63	L	17.5082
1004	R	729	L	7.0101
1005	R	5258.25	L	5.26428
1010	R	5602.5	L	14.3357
1012	R	2254.5	L	12.2234
1017	R	2426.62	L	9.29758
1019	R	617.625	L	7.46943
1021	R	1967.63	L	12.2787
1023	R	1029.38	L	8.52719
1024	R	1184.63	L	42.722
1026	R	1410.75	L	11.6172
1032	R	1572.75	L	86.3565
1033	R	11454.7	L	34.9819
1035	R	1275.75	L	87.4314

The p-value is .000179. **The result was statistically significant at $p < .10$

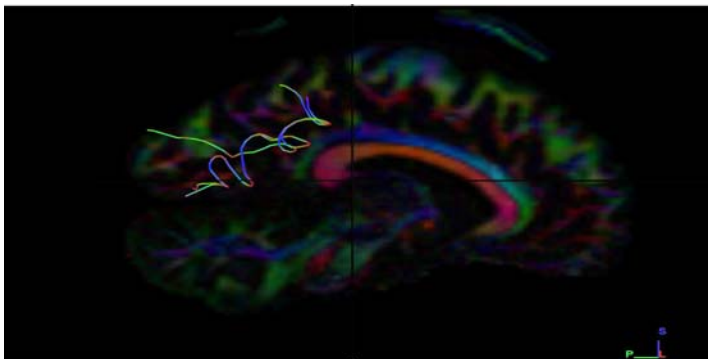

(Fige 10) Sagittal section female right side dataset (1010)

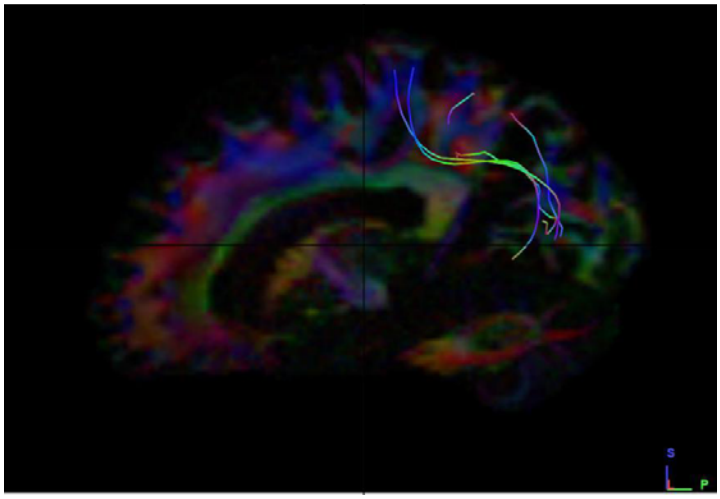

(Fige 11) Sagittal section female left side dataset (1010)

Graphical Representation

(Graph-5) Volume of tracts in female subjects on both left and right sides.

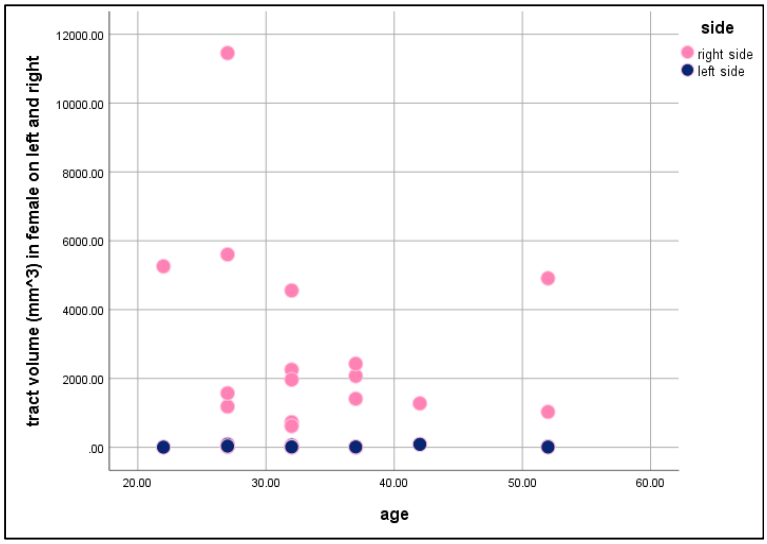

We found that on average, the right side has greater volume of tracts than on left side in female subjects.

c) Volume of Tracts in both Male and Female Left Side

We selected sixteen healthy adult male participants for our study, having a mean age of 30.4 years.

Female:

The volume of tracts was analyzed in 16 female subjects by tracing the neural structural connectivity between the primary visual cortex to Inferior Temporal Lobe,

we found that the female subject (1032) with the mean age of 27 years has highest volume of tracts.

Male:

The volume of tracts were analyzed in 16 male subjects by tracing the neural structural connectivity between the primary visual cortex to Inferior Temporal Lobe, we found that the male subject (1023) with the mean age of 27 has least volume of tracts, (Table 7).

TABLE 7 VOLUME OF TRACTS IN MALE AND FEMALE LEFT**

Female Datasets	Volume of Tracts(mm ^ 3)	Male Datasets	Volume of tracts(mm ^ 3)
1001	0	1006	13.0699
1002	59.3764	1007	11.1297
1003	17.5082	1008	29.3419
1004	7.0101	1009	29.8612
1005	5.26428	1011	3.09596
1010	14.3357	1013	12.7566
1012	12.2234	1014	8.55175
1017	9.29758	1015	9.15248
1019	7.46943	1016	13.6044
1021	12.2787	1022	18.4829
1023	8.52719	1025	0
1024	42.722	1027	11.6117
1026	11.6172	1028	5.31415
1032	86.3565	1029	8.86962
1033	34.9819	1030	8.30297
1035	87.4314	1031	14.6043

The p-value is .073828. **The result was statistically significant at $p < .10$

Graphical Representation

(Grap-6) Graphical representation of volume of tracts in male and female subjects on left sides.

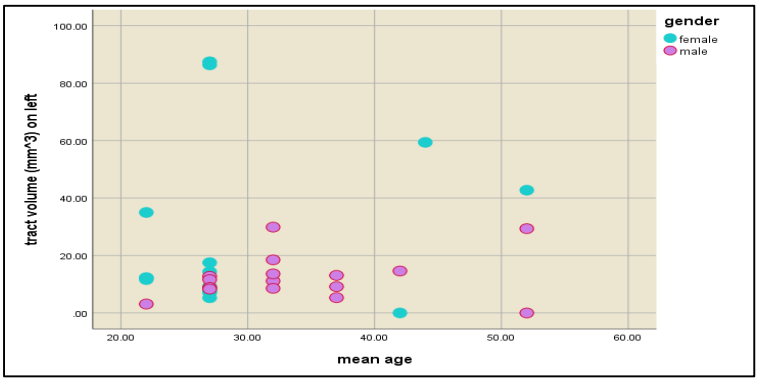

We found that female subjects have greater volume of fibres on left side than in male subjects.

d) Volume of Tracts on both Male and Female Right Side

We selected sixteen healthy adult male participants for our study having a mean age of 30.4 years.

Female:

The volume of tracts was analyzed in 16 female subjects by tracing the neural structural connectivity between the primary visual cortex to Inferior Temporal Lobe, we found that the female subject (1017) with the mean age of 27 years has highest volume of tracts.

Male:

The volume of tracts were analyzed in 16 male subjects by tracing the neural structural connectivity between the primary visual cortex to Inferior Temporal Lobe, we found that the male subject (1005) with the mean age of 27 has least volume of tracts, (Table 8).

TABLE 8 VOLUME OF TRACTS IN MALE AND FEAMLE RIGHT*

Female Datasets	Volume of Tracts(mm ^)	Male Datasets	Volume of tracts(mm ^ 3)
1001	2072.25	1006	712.1251
1002	4556.25	1007	1191.38
1003	4910.63	1008	2203.8

1004	729	1009	5001.75
1005	5258.25	1011	540
1010	5602.5	1013	2683.13
1012	2254.5	1014	3763.13
1017	2426.62	1015	1748.25
1019	617.625	1016	1819.12
1021	1967.63	1022	894.375
1023	1029.38	1025	1545.75
1024	1184.63	1027	2703.38
1026	1410.75	1028	7661.25
1032	1572.75	1029	1144.12
1033	11454.7	1030	8.30297
1035	1275.75	1031	14.6043

The p-value is .294117. *The result was not statistically significant at $p < .10$

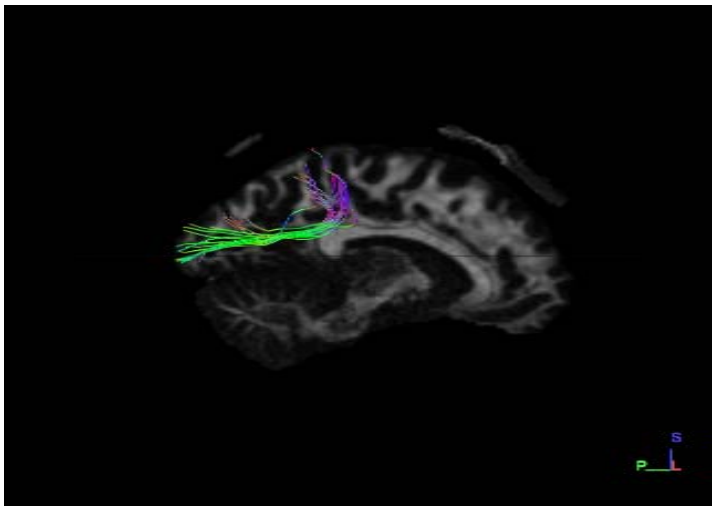

(Fig 12) Sagittal section female right side dataset (1017)

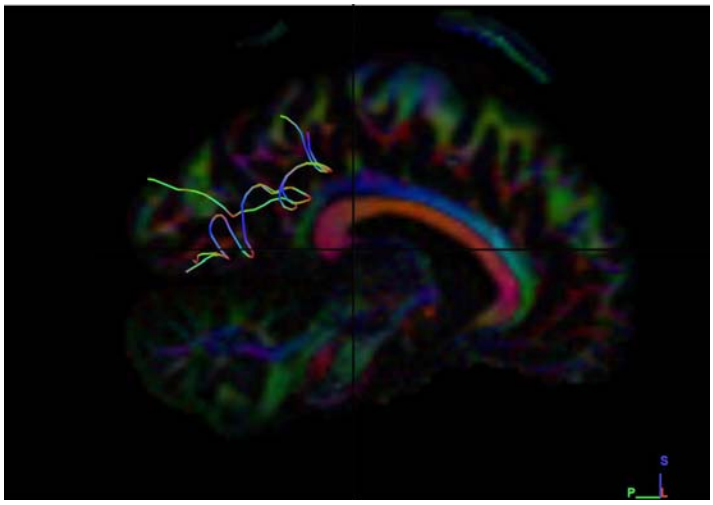

(Fig 13) Sagittal section male right side dataset (1017)

Graphical Representation

(Graph-7) Graphical representation of volume of tracts in male and female subjects on the right side

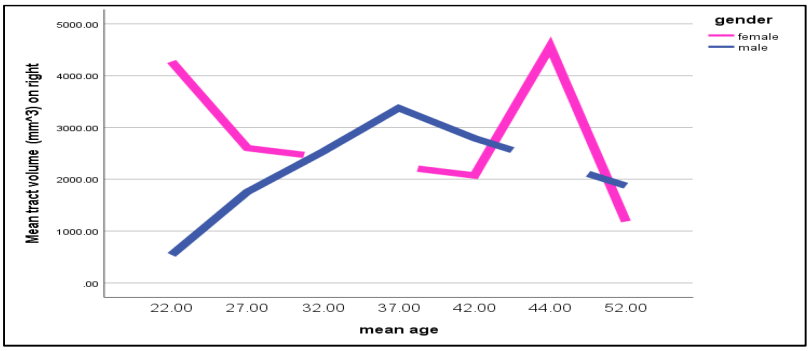

We found that female subjects have greater volume fibers on the right side than male subjects do.

A) Mean Length of Tracts

Tract mean length (mm) the average absolute deviation of a data from a central point. We are analysing tract mean length (mm) present in both the sexes (i) Male subjects and ii) Female subjects. The comparison of Mean Length of Fibers is was done between the seed and the end region under four parameters;

a) Male Right and Left Side

b) Female Right and Left side

c) Right side Male and Female

d) Left side Male and Female

a) Mean Length of Tracts in Male Subjects on both right and left side

We selected sixteen healthy adult male participants for our study, having a mean age of 30.4 years.

Right Side:

The Mean Length of Tracts were analyzed in 16 male subjects by tracing the neural structural connectivity between the primary visual cortex to Inferior Temporal Lobe, we found that the male subject (1008) with the mean age of 57 years having Greater Mean Length of Tracts.

Left Side:

Mean Length of Tracts were analyzed in 16 male subjects by tracing the neural structural connectivity between the primary visual cortex to Inferior Temporal Lobe, we found that the male subject (1007) with the mean age of 57 having least Mean Length of Tracts, (Table 9).

TABLE 9 MEAN LENGTH OF TRACTS MALE RIGHT AND LEFT*

Subjects	SIDE	Mean length of Tracts (mm)	SIDE	Mean length of tracts (mm)
1006	R	69.0259	L	78.0762
1007	R	86.0321	L	51.0098
1008	R	139.547	L	100.312
1009	R	103.704	L	91.8397
1011	R	119.8	L	107.296
1013	R	89.2041	L	111.679
1014	R	96.8163	L	40.6223
1015	R	108.12	L	74.1402
1016	R	104.525	L	76.5809
1022	R	107.692	L	62.3265
1025	R	90.9534	L	79.3537
1027	R	105.144	L	105.24
1028	R	80.9345	L	82.9008

1029	R	94.4569	L	94.1059
1030	R	106.859	L	100.927
1031	R	112.151	L	53.6572

The p-value is .008685. **The result was statistically significant at $p < .10$

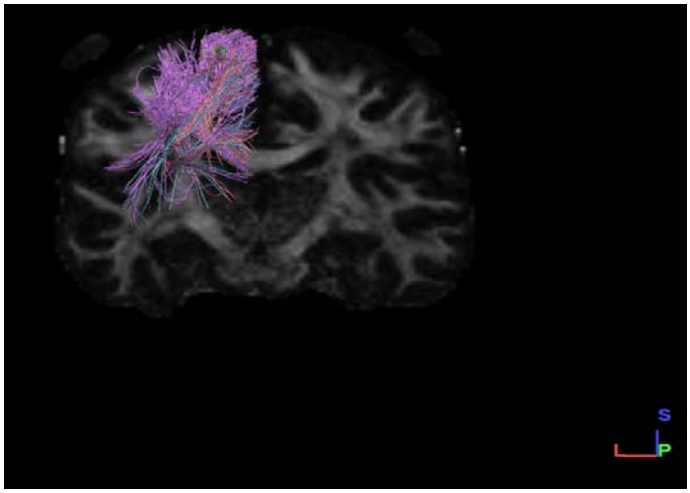

(Fig 14) Coronal section male left side dataset

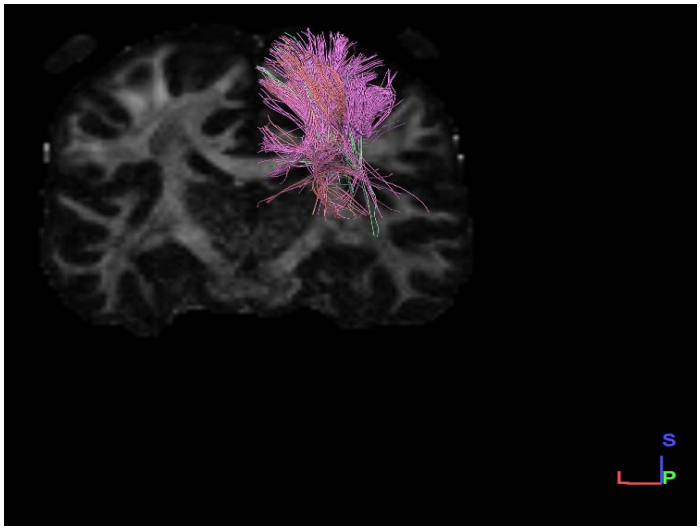

(Fig 15) Coronal section male right side dataset

Graphical Representation

(Graph-8) Graphical representation of mean tract length in on both right and left sides in male subjects.

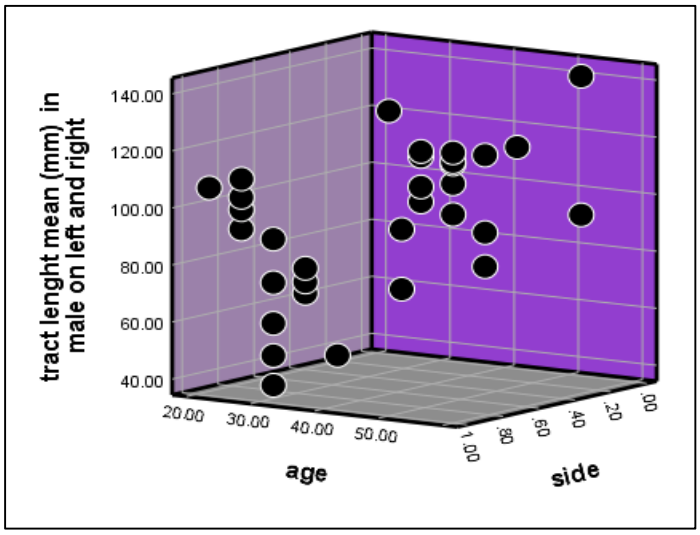

We found that the right side has greater mean tract length than left side in male subjects.

b) Mean Length of Tracts in Female Subjects on both right and left side

We selected sixteen healthy adult female participants for our study having a mean age of 30.4 years.

Right Side:

The mean length of tracts were analyzed in 16 female subjects by tracing the neural structural connectivity between the primary visual cortex to Inferior Temporal Lobe, we found that the female subject (1004) with the mean age of 45 years having greater mean length of tracts.

Left Side:

Mean length of tracts were analyzed in 16 female subjects by tracing the neural structural connectivity between the primary visual cortex to Inferior Temporal Lobe, we found that the female subject (1001) with the mean age of 41.4 having least mean length of tracts, (Table 10).

TABLE 10 MEAN LENGTH OF TRACTS IN FEMALE RIGHT AND LEFT*

Subjects	SIDE	Mean length of Tracts (mm)	SIDE	Mean length of tracts (mm)
1001	R	91.944	L	50.4651

1002	R	92.1148	L	115.22
1003	R	94.0607	L	86.675
1004	R	76.2553	L	111.524
1005	R	99.1371	L	47.9897
1010	R	93.7265	L	73.2423
1012	R	95.3105	L	89.1171
1017	R	89.0993	L	52.3645
1019	R	96.8738	L	94.3324
1021	R	90.1429	L	98.6967
1023	R	101.393	L	38.6527
1024	R	85.886	L	120.831
1026	R	102.519	L	57.9078
1032	R	86.3565	L	1572.75
1033	R	90.9583	L	92.3496
1035	R	87.4314	L	1275.75

The p-value is .186217. *The result was statistically *not* significant at $p < .10$

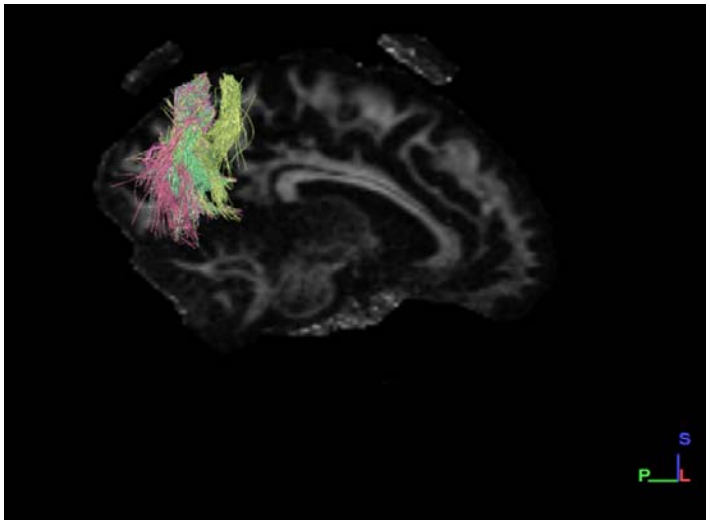

(Fig 16) Sagittal section female right side dataset

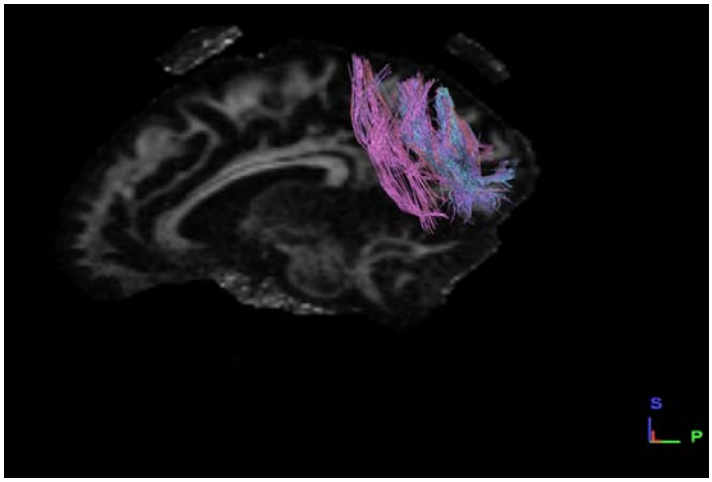

(Fig 17) Sagittal section female left side dataset

Graphical Representation

(Graph-9) Graphical representation of mean tract length in on both right and left sides in female subjects.

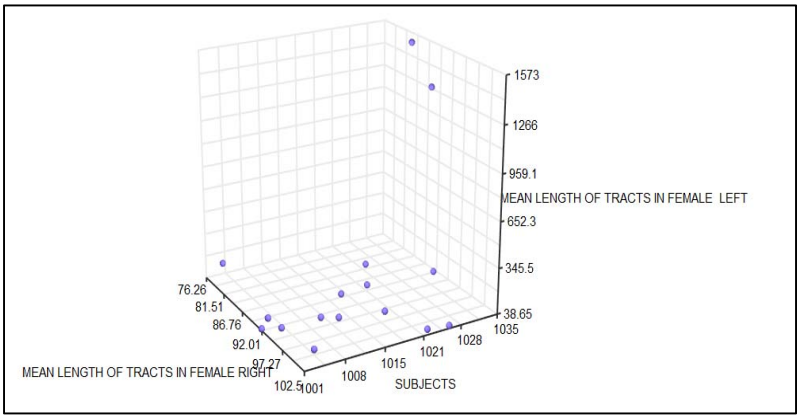

We found that the right side is having greater number of tracts than left side in female subjects.

c) Mean Length of Tracts both Male and Female Left Side

We selected sixteen healthy adult male and female participants for our study having a mean age of 30.4 years.

Male:

The mean length of tracts were analyzed in 16 male subjects by tracing the neural structural connectivity between the primary visual cortex to Inferior Temporal Lobe, we found that the male subject (1008) with the mean age of 57 years having greater mean length of tracts.

Female:

Mean Length of Tracts were analyzed in 16 female subjects by tracing the neural structural connectivity between the primary visual cortex to Inferior Temporal Lobe, we found that the female subject (1004) with the mean age of 27 having least mean length of tracts, (Table 11).

TABLE 11 MEAN LENGTH OF TRACTS MALE AND FEMALE RIGHT**

Female Datasets	Mean length of Tracts (mm)	Male Datasets	Mean length of tracts (mm)
1001	91.944	1006	69.0259
1002	92.1148	1007	86.0321
1003	94.0607	1008	139.547
1004	76.2553	1009	103.704
1005	99.1371	1011	119.8
1010	93.7265	1013	89.2041
1012	95.3105	1014	96.8163
1017	89.0993	1015	108.12
1019	96.8738	1016	104.525
1021	90.1429	1022	107.692
1023	101.393	1025	90.9534
1024	85.886	1027	105.144
1026	102.519	1028	80.9345
1032	86.3565	1029	94.4569
1033	90.9583	1030	106.859
1035	87.4314	1031	112.151

The p-value is .05493. **The result was statistically significant at $p < .10$

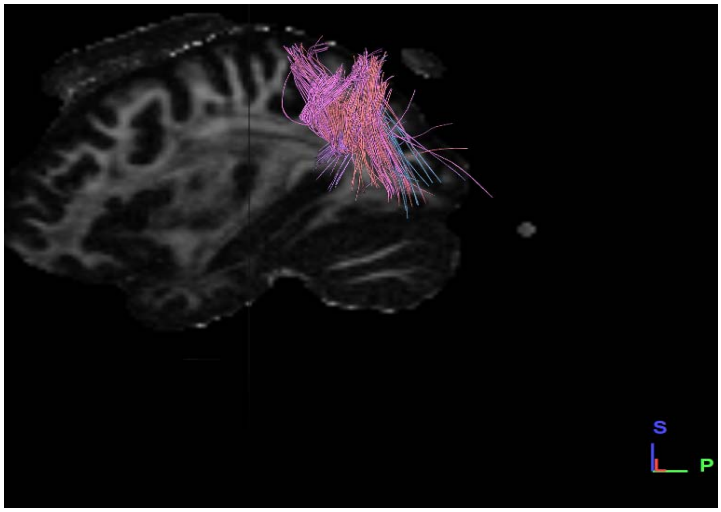

(Fig 18) Sagittal section female right side dataset

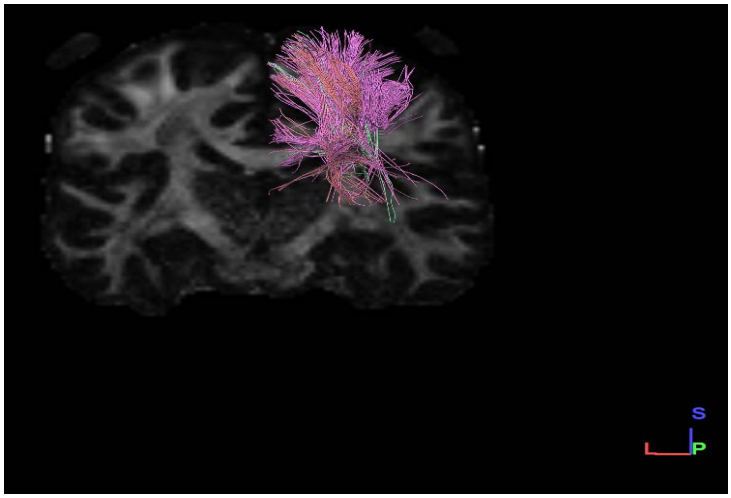

(Fig 19) Coronal section male right side dataset

Graphical Representation

(Graph-10) Graphical representation of mean tract length in both male and female subjects on right side.

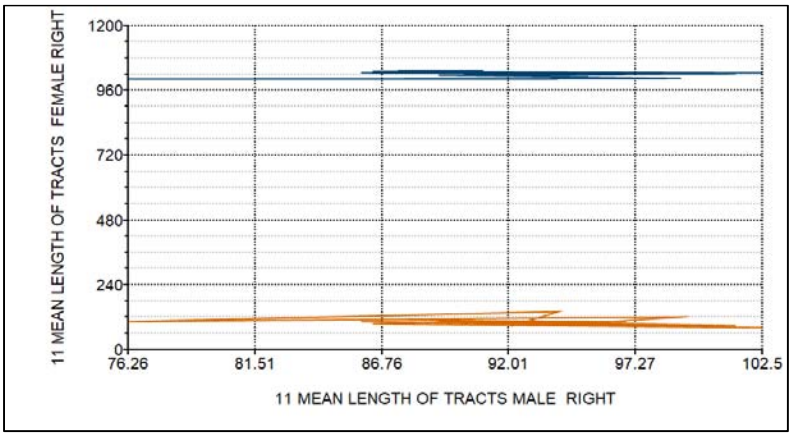

We found that the male subjects have greater mean length of tract fibres on right side than female subjects.

d) Mean Length of Tracts both Male and Female Right Side

We selected sixteen healthy adults male and female participants for our study having a mean age of 30.4 years.

Male:

The Mean Length of Tracts were analyzed in 16 male subjects by tracing the neural structural connectivity between the primary visual cortex to Inferior Temporal Lobe, we found that the male subject (1032) with the mean age of 27 years having Greater Mean Length of Tracts.

Female:

Mean Length of Tracts were analyzed in 16 female subjects by tracing the neural structural connectivity between the primary visual cortex to Inferior Temporal Lobe, we found that the female subject (1007) with the mean age of 27 having least Mean Length of Tracts, (Table12).

TABLE 12 MEAN LENGTH OF TRACTS MALE AND FEMALE LEFT*

Female Datasets	Mean length of Tracts (mm)	Male Datasets	Mean length of tracts (mm)
1001	50.4651	1006	78.0762
1002	115.22	1007	51.0098
1003	86.675	1008	100.312
1004	111.524	1009	91.8397
1005	47.9897	1011	107.296
1010	73.2423	1013	111.679
1012	89.1171	1014	40.6223
1017	52.3645	1015	74.1402
1019	94.3324	1016	76.5809
1021	98.6967	1022	62.3265
1023	38.6527	1025	79.3537

1024	120.831	1027	105.24
1026	57.9078	1028	82.9008
1032	1572.75	1029	94.1059
1033	92.3496	1030	100.927
1035	1275.75	1031	89.0411

The p-value is .165737. *The result was statistically *not* significant at $p < .10$.

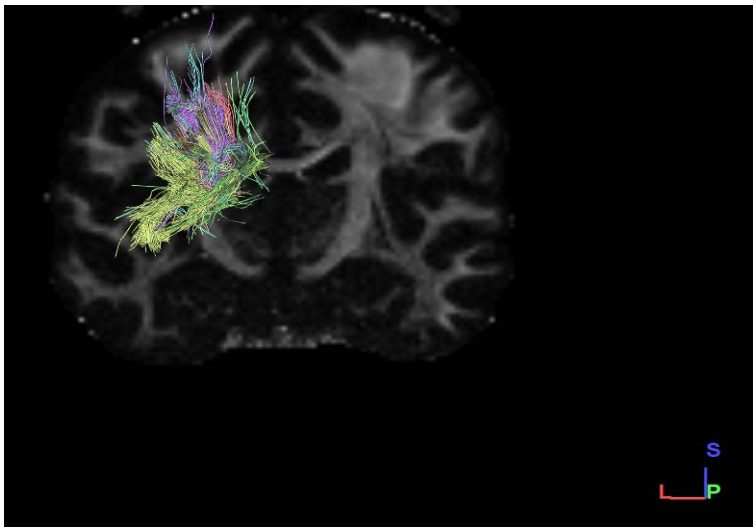

(Fig 20) Coronal section male left side dataset

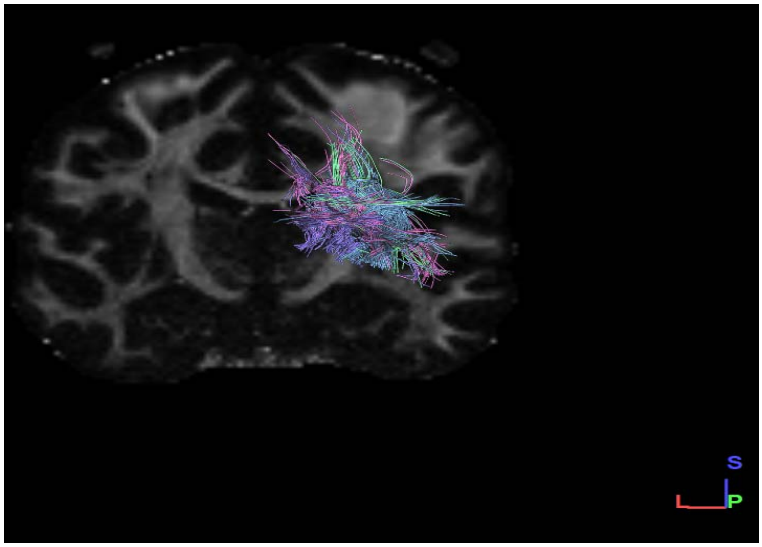

(Fig 21) Coronal section Female left side dataset

Graphical Representation

(Grap-11) Graphical representation of mean tract length in both male and female subjects on left side.

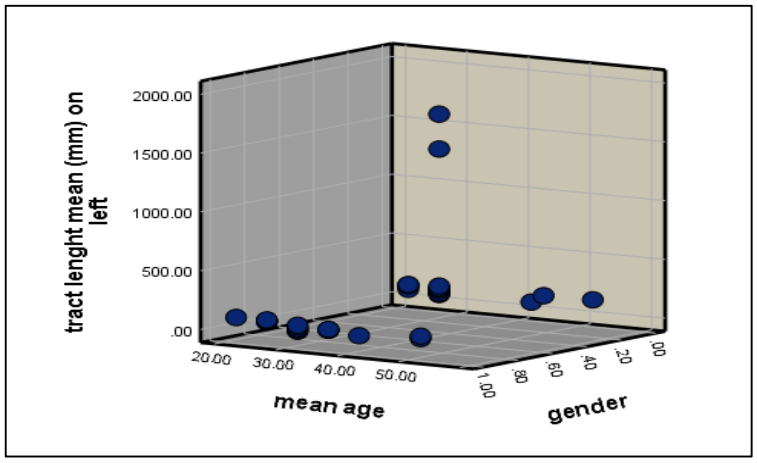

We found that the male subjects have greater mean tract length of fibers on left side than female subjects.

D) Tracts Length Standard Deviation

a) Tract length standard deviation in male subjects on right and left side

We selected sixteen healthy adult male participants for our study, having a mean age of 30.4 years.

Right Side:

The Tract length standard deviation were analyzed in 16 male subjects by tracing the neural structural connectivity between the primary visual cortex to Inferior Temporal Lobe, we found that the male subject (1009) with the mean age of years has least tract length standard deviation.

Left Side:

Tract length standard deviation were analyzed in 16 male subjects by tracing the neural structural connectivity between the primary visual cortex to Inferior Temporal Lobe, we found that the male subject (1029) with the mean age of having highest tract length standard deviation, (Table 13).

TABLE 13 TRACT LENGTH STANDARD DEVIATION IN MALE RIGHT AND LEFT**

Subjects	SIDE	Tract length Standard Deviation (mm)	SIDE	Tract Length Standard Deviation (mm)
1006	R	6.930905	L	384.75
1007	R	6.96374	L	3979.13
1008	R	56.5733	L	1056.38
1009	R	14.1887	L	1056.38
1011	R	2.77598	L	1515.37
1013	R	6.5704	L	2095.87
1014	R	7.2153	L	1613.25
1015	R	7.553	L	2433.37
1016	R	8.40032	L	2673
1022	R	5.42159	L	1113.75
1025	R	7.11046	L	185.625
1027	R	9.54942	L	2325.38
1028	R	7.78756	L	2801.25
1029	R	5.83931	L	3425.63
1030	R	5.21735	L	3013.88
1031	R	8.51525	L	843.75

The p-value is $< .00001$.** The result was statistically significant at $p < .10$

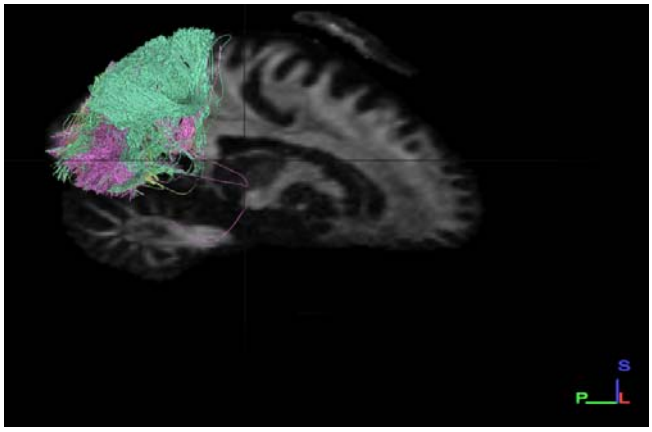

(Fig 22) Sagittal section male right side dataset

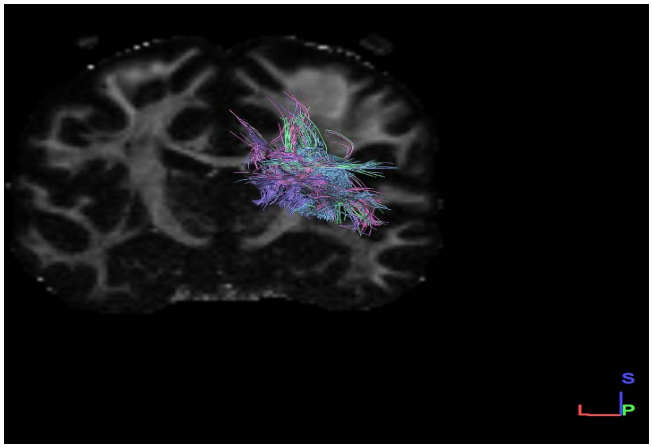

(Fig 23) Coronal section male left side dataset

Graphical Representation

(Graph-12) Graphical representation of tract length standard deviation on both right and left sides in male subjects.

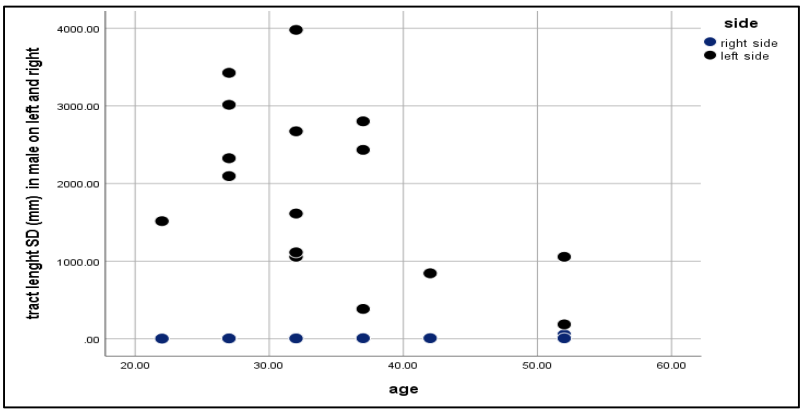

We found that male subjects have greater tracts length standard deviation on left side than on right side.

b) Tract Length Standard Deviation in Female subjects on both Right and Left Sides

We selected sixteen healthy adult male participants for our study, having a mean age of 30.4 years.

Right Side:

The Tract length standard deviation were analyzed in 16 female subjects by tracing the neural structural connectivity between the primary visual cortex to Inferior

Temporal Lobe, we found that the female subject have least tract standard deviation on right side (1007).

Left Side:

Tract length standard deviation were analyzed in 16 female subjects by tracing the neural structural connectivity between the primary visual cortex to Inferior Temporal Lobe, we found least tract length standard deviation in female subjects on the right side (1007), (Table 14).

TABLE 14 TRACT LENGTH STANDARD DEVIATION IN FEMALE RIGHT AND LEFT**

Subjects	SIDE	Tract length Standard Deviation (mm)	SIDE	Tract Length Standard Deviation (mm)
1001	R	7.76203	L	118.125
1002	R	7.02543	L	8032.5
1003	R	8.47677	L	9321.75
1004	R	8.99159	L	2956.5
1005	R	7.96865	L	1117.12
1010	R	8.73392	L	853.875
1012	R	7.25344	L	421.875
1017	R	12.0259	L	3931.87
1019	R	4.68937	L	3894.75
1021	R	4.57601	L	4131
1023	R	7.43073	L	2953.13
1024	R	6.25829	L	1420.88
1026	R	6.32936	L	3628.13
1032	R	4.8742	L	4.8742
1033	R	9.60303	L	1917
1035	R	6.07921	L	6.07921

The p-value is .000317. **The result was statistically significant at $p < .10$

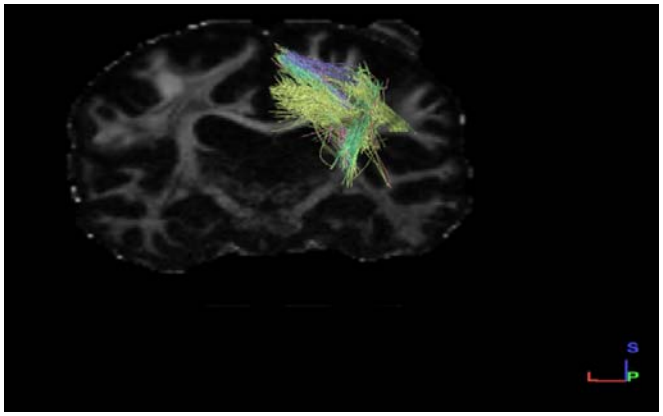

(Fig 24) Coronal section Female right side dataset

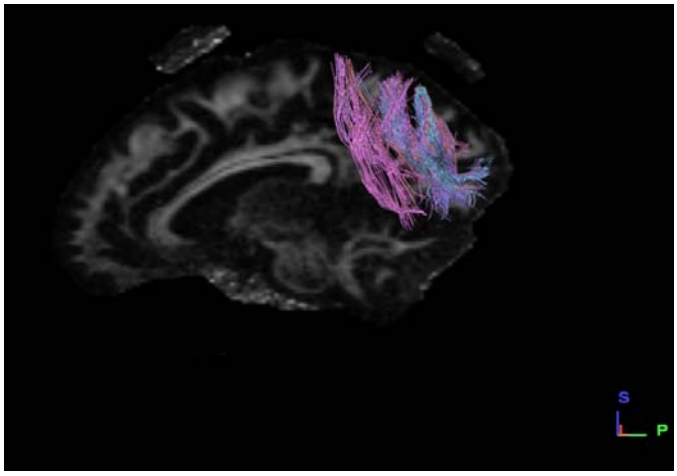

(Fig25) Sagittal section Female left side dataset

Graphical Representation

(Graph-13) Graphical representation of tract length standard deviation on both right and left sides in female subjects.

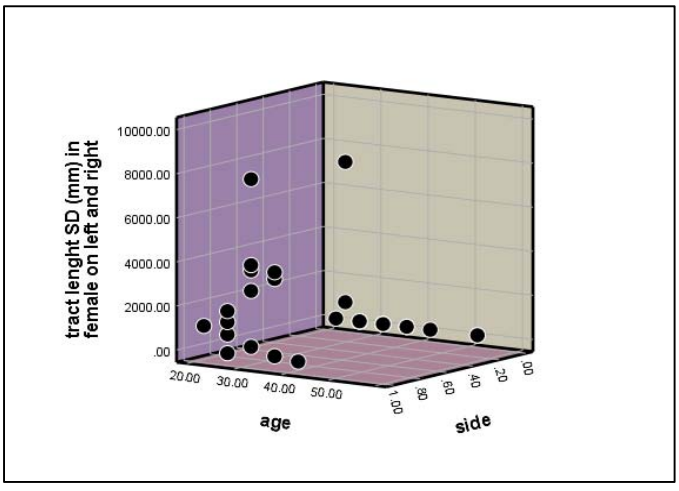

We found that left side of female subjects has greater tract length standard deviation than right side.

c) Tract Length Standard Deviation in both Male and Female Right Side

Male:

The tract length standard deviation was analyzed in 16 male subjects by tracing the neural structural connectivity between the primary visual cortex to Inferior Temporal Lobe, we found that the male subject (1008) with the mean age of 57 years has greater mean length of tracts.

Female:

The tracts length standard deviation were analyzed in 16 female subjects by tracing the neural structural connectivity between the primary visual cortex to Inferior Temporal Lobe, we found that the female subject (1021) with the mean age of 27 having least mean length of tracts, (Table 9).

TABLE 15 TRACT LENGTH STANDARD DEVIATION MALE AND FEMALE AT RIGHT*

Female datasets	Tract length Standard Deviation (mm)	Male Datasets	Tract Length Standard Deviation (mm)
1001	7.76203	1006	6.930905
1002	7.02543	1007	6.96374
1003	8.47677	1008	56.5733
1004	8.99159	1009	14.1887
1005	7.96865	1011	2.77598
1010	8.73392	1013	6.5704
1012	7.25344	1014	7.2153
1017	12.0259	1015	7.553
1019	4.68937	1016	8.40032
1021	4.57601	1022	5.42159
1023	7.43073	1025	7.11046
1024	6.25829	1027	9.54942
1026	6.32936	1028	7.78756

1032	4.8742	1029	5.83931
1033	9.60303	1030	5.21735
1035	6.07921	1031	8.51525

The p-value is .346856. *The result was statistically *not* significant at $p < .10$

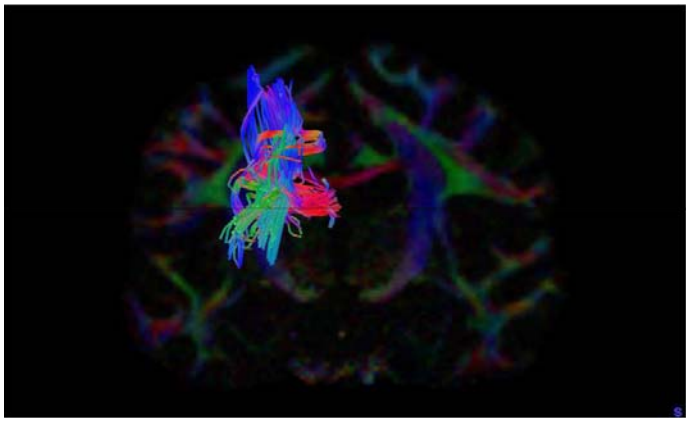

(Fig 26) Coronal section male left side dataset

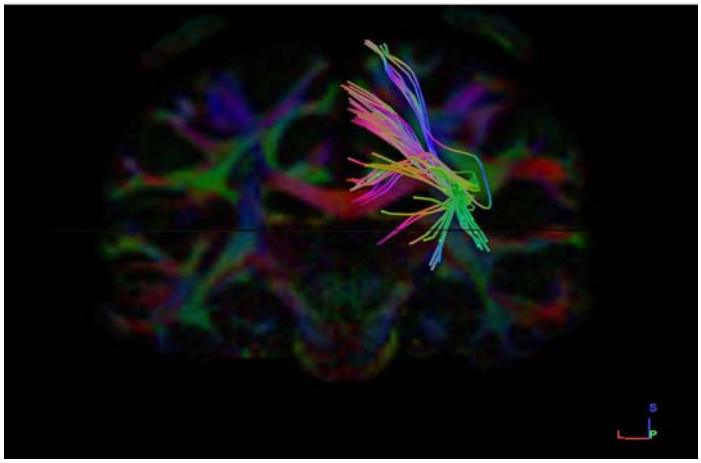

(Fig 27) Coronal section female right side dataset

Graphical Representation

(Graph-14) Graphical representation of tract length standard deviation on right side in male and female subjects.

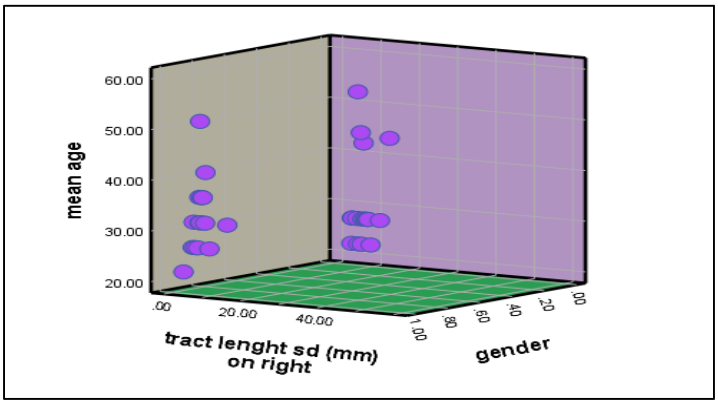

We found that male subjects have greater tract length standard deviation on right side than female subjects.

d) The Tract Length Standard Deviation both Male and Female Left Side

Male:

The tract length standard deviation was analyzed in 16 male subjects by tracing the neural structural connectivity between the primary visual cortex to Inferior Temporal Lobe, we found that the male subject (1001) with the mean age of 42 years having least Mean Length of Tracts.

Female:

Tract length standard deviation were analyzed in 16 female subjects by tracing the neural structural connectivity between the primary visual cortex to Inferior Temporal Lobe, we found that the female subject (1003) with the mean age of 27 has greater Mean Length of Tracts, (Table 9).

TABLE 16 TRACT LENGTH STANDARD DEVIATION IN MALE AND FEMALE AT LEFT *

Female datasets	Tract length Standard Deviation (mm)	Male Datasets	Tract Length Standard Deviation (mm)
1001	118.125	1006	384.75
1002	8032.5	1007	3979.13
1003	9321.75	1008	1056.38
1004	2956.5	1009	1056.38
1005	1117.12	1011	1515.37
1010	853.875	1013	2095.87

1012	421.875	1014	1613.25
1017	3931.87	1015	2433.37
1019	3894.75	1016	2673
1021	4131	1022	1113.75
1023	2953.13	1025	185.625
1024	1420.88	1027	2325.38
1026	3628.13	1028	2801.25
1032	4.8742	1029	3425.63
1033	1917	1030	3013.88
1035	6.07921	1031	843.75

The p-value is .239442. *The result was statistically *not* significant at $p < .10$.

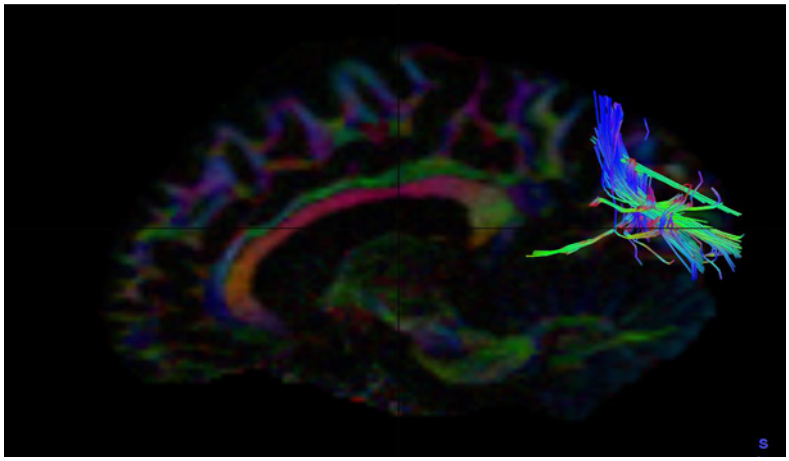

(Fig28) Sagittal section male left side dataset

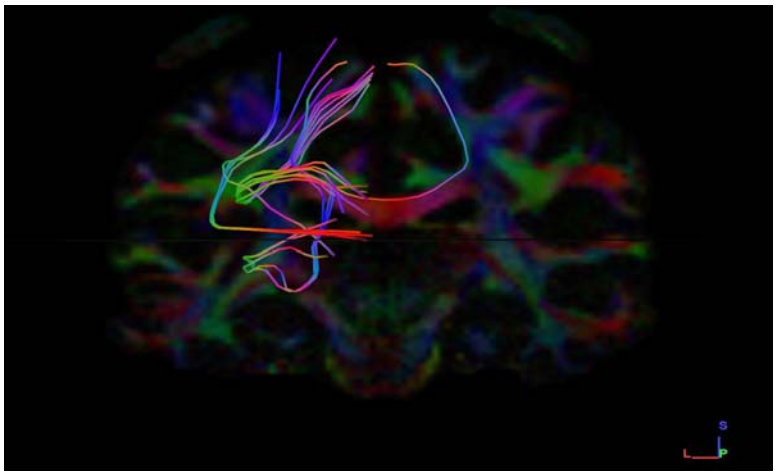

(Fig 29) Coronal section Female left side dataset

Graphical Representation

(Graph-15) Graphical representation of tract length standard deviation on both right and left sides in male subjects.

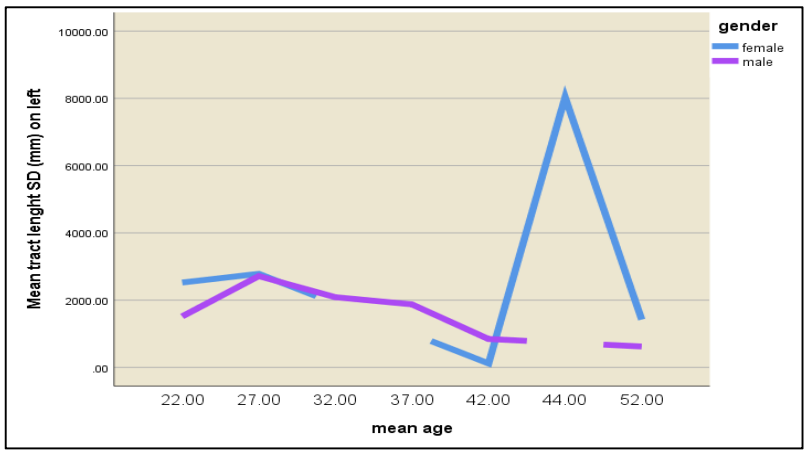

We found that female subjects have a greater tract length standard deviation than in male subjects on left side.

DISCUSSION AND CONCLUSION

The Dorsal (Occipitoparietal) pathway is a part of the dual stream visual brain theory where fibers span from the primary visual cortex to the parietal lobe. The dorsal stream is incapable of visual memory and is affiliated with "on line" control of actions and the spatial localization of stimuli and visual guidance of motor actions; "where?" and "how?" visuospatial discrimination [9]. With the use of Diffusion Tensor Magnetic Resonance Imaging Tractography, we were able to study the structural connections of the primary visual cortex (V1) to the Superior Parietal lobe in efforts to relate its clinical and functional significance [10]. "Skilled grasp can be defined as hand movements requiring independent control of each finger, which has been shown to rely on a highly developed corticospinal tract (Lemon, 2008)" [9]. When reaching out to grasp an object, the interpretation of sensory information is critical in accurately performing the action in terms of adaptation to the size and location of the object [11], [13], [15]. The object has to be visually distinguished before commencing the desired motion that would be executed into the motor action plan. Fibers of the occipitoparietal pathway projects to premotor areas PMv and PMd (Polanena.VDavare.M (2015) allows for visual guidance in the performance of skilled

hand movements [9]. As such, lesions of the fibers in the dorsal stream (Posterior Parietal Cortex) would negatively influence spatial perplexity of individuals characterized by a deficit in the acuity of relative loci and the localization of objects during targeted actions resulting in Optic ataxia [11]. Optic ataxia is a neurodegenerative disorder that is prevalent in patients suffering from Alzheimer's disease (Posterior cortical atrophy- the visual variant of Alzheimer's disease) in which there is a higher order visual dysfunction. Optic ataxia is a part of the triad of neurophysiological impairments in Balint's Syndrome in which there is a loss of the ability to coordinate manual movements [11], [12], [14]. In relation, lesions to the Posterior Parietal Cortex (PPC) would result in patients having a loss of the ability to coordinate manual movements in reference to their peripheral visual camp hence development of Optic Ataxia due to the inability to be visually guided by the dorsal stream visual pathway [13]. Patients therefore would not only encounter difficulty in performing low resolution spatially accurate reaches, but would also experience challenges when trying to adjust their hand posture in reaching out to grasp objects of varying alignment or size [15]. For example, in a case that a patient has a lesion in parietal posterior cingulate (lesion before the optic decussation), that patient would think that his hand is loose but he does not realize that he cannot coordinate his fine hand movements beyond the nasal camp on the affected visual site. We now conclude the findings of this study by stating; the current observations propose further insights to understand the structural existence and functional correlations for visuo-motor coordination pathway or "how" stream pathways in visual perception. Damage to this "how "stream fibers in the Visual pathways, manifest as Optic ataxia in Alzheimer's Patients. However, these findings need to be confirmed with functional MRIs analysis in future understandings for better understanding of its significance in other neurodegenerative diseases and how this finding can affect future diagnostic and treatment approaches in these disorders.

REFERENCES

[1] Wright, M. J. (1969). **Visual Receptive Fields of Cells in a Cortical Area remote from the Striate Cortex in the Cat**. *Nature, 223(5209), 973-975. doi:10.1038/223973a0.* Retrieved; 02/05/2018.

[2] Regan, D., & Heron, J. R. (1969). **Clinical investigation of lesions of the visual pathway: A new objective technique**. *Journal of Neurology, Neurosurgery & Psychiatry, 32(5), 479-483. doi:10.1136/jnnp.32.5.479.* Retrieved; 20/06/2018.

[3] Allman, J. M., & Kaas, J. H. (1971). **Representation of the visual field in striate and adjoining cortex of the owl monkey(Aotus trivirgatus)**. *Brain Research, 35(1), 89-106. doi:10.1016/0006-8993(71)90596-8.* Retrieved; 09/04/2018.

[4] Haaxma, R., & Kuypers, H. G. (1975). **Intrahemispheric Cortical Connexions And Visual Guidance Of Hand And Finger Movements In The Rhesus Monkey**. *Brain, 98(2), 239-260. doi:10.1093/brain/98.2.239.* Retrieved; 12/05/2018.

[5] Seltzer, B., & Pandya, D. N. (1978). **Afferent cortical connections and architectonics of the superior temporal sulcus and surrounding cortex in the rhesus monkey**. *Brain Research, 149(1), 1-24. doi:10.1016/0006-8993(78)90584-x.* Retrieved; 30/03/2018.

[6] Leinonen, L., HyvRinen, J., Nyman, G., & Linnankoski, I. (1979). **I. Functional properties of neurons in lateral part of associative area 7 in awake monkeys**. *Experimental Brain Research,34(2). doi:10.1007/bf00235675.* Retrieved; 06/04/2018.

[7] Baker, J. F., Petersen, S. E., Newsome, W. T., & Allman, J. M. (1981). **Visual response properties of neurons in four extrastriate visual areas of the owl monkey (Aotus trivirgatus): A quantitative comparison of medial, dorsomedial, dorsolateral, and middle temporal areas**. *Journal of Neurophysiology, 45(3), 397-416. doi:10.1152/jn.1981.45.3.397.* Retrieved; 11/06/2018.

[8] Freiwald, W. (2013). **Faculty of 1000 evaluation for Visual properties of neurons in a polysensory area in superior temporal sulcus of the macaque**. *F1000 - Post-publication Peer Review of the Biomedical Literature. doi:10.3410/f.717989827.793472996.* Retrieved; 02/07/2018.

[9] Davare, M., & Polanen, V., (2015). **Interactions between dorsal and ventral streams for controlling skilled grasp.** Neurophysiologia. https://doi.org/10.1016/j.neuropsychologia.2015.07.010. Retrieved:10/04/2018.

[10] Rokem, A., Takemura, H., & Bock, S. A., (2017). **The visual white matter: The application of diffusion MRI and fiber tractography to vision science.** Journal of vision. doi:10.1167/17.2.4. Retrieved:09/04/2018.

[11] Honeycutt, F. Claire., Kharouta, M., & Perreault, J. Eric., (2013). **Evidence for reticulospinal contributions to coordinated finger movements in humans**. Journal of neurophysiology. doi:10.1152/jn.00866.2012. Retrieved:09/04/2018.

[12] Halasz, V., & Cunnington, R., (2012). **Unconscious Effects of Action on Perception.** Brain Sciences. doi:10.3390/brainsci2020130. Retrieved:09/04/2018.

[13] Pratesi, C. Cristiana., Connolly, D. Jason., & Milner, D. A., (2013). **Optic ataxia as a model to investigate the role of the posterior parietal cortex in visually guided action: evidence from studies of patient M.H**.Frontiers in Human Neurosciences. doi:10.3389/fnhum.2013.00336. Retrieved: 10/04/2018.

[14] Andersan, A. Richard., Andersan, N. Kristen., Hwang, J. Eun., & Hauschild, M., (2014). **Optic ataxia: from Balint's syndrome to the parietal reach region**.Neuron. doi: 10.1016/j.neuron.2014.02.025. Retrieved: 10/04/2018.

[15] Miriam, G. Simon., & Conway, L., (2014). **Reach-to-precision grasp deficits in amblyopia: Effects of object contrast and low visibility.** https://doi.org/10.1016/j.visres.2014.11.009. Retrieved: 09/04/2018.

[16] Fan, Q., Witzel, T., Nummenmaa, A., (2016). ***MGH–USC Human Connectome Project datasets with ultra-high b-value diffusion MRI.*** *Neuroimage.* doi.org/10.1016/j.neuroimage.2015.08.075. Retrieved 06/05/2018

[17] Taira, M., Mine, S., Georgopoulos, A., Murata, A., & Sakata, H. (1990). Parietal cortex neurons of the monkey related to the visual guidance of hand movement. Experimental Brain Research, 83(1). doi:10.1007/bf00232190. Retrieved; 15/05/2018.

[18] Mowry, C., Pimentel, A., Sparks, E., & Hanlon, B. (2013). Materials characterization activities for "Take Our Sons&Daughters to Work Day" 2013. doi:10.2172/1096449. Retrieved; 06/04/2018.

[19] 1Haxby, J. V., Grady, C. L., Horwitz, B., Salerno, J., Ungerleider, L. G., Mishkin, M., & Schapiro, M. B. (1993). Dissociation of Object and Spatial Visual Processing Pathways in Human Extrastriate Cortex. Functional Organisation of the Human Visual Cortex, 329-340. doi:10.1016/b978-0-08-042004-2.50028-9. Retrieved; 30/03/2018.

[20] Goodale, M. A., & Milner, A. (1992). Separate visual pathways for perception and action. Trends in Neurosciences, 15(1), 20-25. doi:10.1016/0166-2236(92)90344-8. Retrieved; 10/06/2018.

[21] Mcintosh, A., Grady, C., Ungerleider, L., Haxby, J., Rapoport, S., & Horwitz, B. (1994). Network analysis of cortical visual pathways mapped with PET. The Journal of Neuroscience, 14(2), 655-666. doi:10.1523/jneurosci.14-02-00655.1994. Retrieved; 09/06/2018.

[22] Faillenot, I. (1997). Visual pathways for object-oriented action and object recognition: Functional anatomy with PET. Cerebral Cortex, 7(1), 77-85. doi:10.1093/cercor/7.1.77. Retrieved; 08/07/2018.

[23] Deubel, H., Schneider, W. X., & Paprotta, I. (1998). Selective Dorsal and Ventral Processing: Evidencfor a Common Attentional Mechanism in Reaching and Perception. Visual Cognition,5(1-2), 81-107. doi:10.1080/713756776. Retrieved; 17/05/2018.

[24] Desimone, R. (1998). Visual attention mediated by biased competition in extrastriate visual cortex. Philosophical Transactions of the Royal Society B: Biological Sciences,353(1373), 1245-1255. doi:10.1098/rstb.1998.0280. Retrieved; 06/04/2018.

[25] Grill-Spector, K., Kushnir, T., Edelman, S., Itzchak, Y., & Malach, R. (1998). Cue-Invariant Activation in Object-Related Areas of the Human Occipital

Lobe. Neuron,21(1), 191-202. doi:10.1016/s0896-6273(00)80526-7. Retrieved; 20/05/2018.

[26] Sabine Kastner And Leslie G. Ungerleider. (2000). Mechanisms of Visual Attention in the Human Cortex. Annual Review of Neuroscience,23(1), 315-341. doi:10.1146/annurev.neuro.23.1.315. Retrieved; 16/05/2018.

[27] Glickstein, M. (2000). How are visual areas of the brain connected to motor areas for the sensory guidance of movement? Trends in Neurosciences,23(12), 613-617. doi:10.1016/s0166-2236(00)01681-7. Retrieved; 12/06/2018.

[28] Pisella, L., Gréa, H., Tilikete, C., Vighetto, A., Desmurget, M., Rode, G., . . . Rossetti, Y. (2000). An'automatic pilot' for the hand in human posterior parietal cortex: Toward reinterpreting optic ataxia. Nature Neuroscience,3(7), 729-736. doi:10.1038/76694. Retrieved; 06/07/2018.

[29] Amedi, A., Malach, R., Hendler, T., Peled, S., & Zohary, E. (2001). Visuo-haptic object-related activation in the ventral visual pathway. Nature Neuroscience,4(3), 324-330. doi:10.1038/85201. Retrieved; 23/05/2018.

[30] Conway, B. R. (2001). Spatial Structure of Cone Inputs to Color Cells in Alert Macaque Primary Visual Cortex (V-1). The Journal of Neuroscience,21(8), 2768-2783. doi:10.1523/jneurosci.21-08-02768.2001. Retrieved; 11/05/2018.

[31] Sigala, N., & Logothetis, N. K. (2002). Visual categorization shapes feature selectivity in the primate temporal cortex. Nature,415(6869), 318-320. doi:10.1038/415318a. Retrieved; 06/07/2018.

[32] Hamed, S. B. (2002). Visual Receptive Field Modulation in the Lateral Intraparietal Area during
Attentive Fixation and Free Gaze. Cerebral Cortex,12(3), 234-245. doi:10.1093/cercor/12.3.234. Retrieved; 12/06/2018.

[33] James, T. W., Humphrey, G., Gati, J. S., Menon, R. S., & Goodale, M. A. (2002). Differential Effects of
Viewpoint on Object-Driven Activation in Dorsal and Ventral Streams. Neuron,35(4), 793-801. doi:10.1016/s0896-6273(02)00803-6. Retrieved; 25/06/2018.

[34] Parallel processing of information in the visual pathways: A general principle of sensory coding?
(2003, March 05). Retrieved fromhttps://www.sciencedirect.com/science/article/pii/0166223682902375. Retrieved; 27/04/2018.

[35] Krauzlis, R. J., & Carello, C. D. (2003). Going for the goal. Nature Neuroscience,6(4), 332-333.
doi:10.1038/nn0403-332. Retrieved; 28/05/2018.

[36] Zhong, Y. (2003). Inferior Parietal Lobule Projections to Anterior Inferotemporal Cortex (Area TE) in Macaque Monkey. Cerebral Cortex,13(5), 527-540. doi:10.1093/cercor/13.5.527. Retrieved; 06/06/2018.

[37] Tootell, R. B., Tsao, D., & Vanduffel, W. (2003). Neuroimaging Weighs In: Humans Meet Macaques in "Primate" Visual Cortex. The Journal of Neuroscience,23(10), 3981-3989. doi:10.1523/jneurosci.23-10- 03981.2003. Retrieved; 18/05/2018.

[38] Rizzolatti, G., & Matelli, M. (2003). Two different streams form the dorsal visual system: Anatomy and functions. Experimental Brain Research,153(2), 146-157. doi:10.1007/s00221-003-1588-0. Retrieved;11/06/2018.

[39] Chatterjee, S., & Callaway, E. M. (2003). Parallel colour-opponent pathways to primary visual cortex. Nature,426(6967), 668-671. doi:10.1038/nature02167. Retrieved; 03/07/2018.

[40] Milner, A., & Goodale, M. (2008). Two visual systems re-viewed. Neuropsychologia,46(3), 774-785. doi:10.1016/j.neuropsychologia.2007.10.005. Retrieved; 11/06/2018.

[41] Claeys, K. G. (2004). Color Discrimination Involves Ventral and Dorsal Stream Visual Areas. Cerebral Cortex,14(7), 803-822. doi:10.1093/cercor/bhh040. Retrieved; 25/05/2018.

[42] Valyear, K. F., Culham, J. C., Sharif, N., Westwood, D., & Goodale, M. A. (2006). A double dissociation between sensitivity to changes in object identity and object orientation in the ventral and dorsal visual streams: A human fMRI study. Neuropsychologia,44(2), 218-228. doi:10.1016/j.neuropsychologia.2005.05.004. Retrieved; 09/06/2018.

[43] Ungerleider, L., & Pessoa, L. (2008). What and where pathways. Scholarpedia,3(11), 5342. doi:10.4249/scholarpedia.5342. Retrieved; 06/04/2018.

[44] Bassi, L., Ricci, D., Volzone, A., Allsop, J. M., Srinivasan, L., Pai, A., . . . Counsell, S. J. (2008). Probabilistic diffusion tractography of the optic radiations and visual function in preterm infants at term equivalent age. Brain, 131(2), 573582. doi:10.1093/brain/awm327. Retrieved; 19/05/2018.

[45] Cohen, L., Dehaene, S., Vinckier, F., Jobert, A., & Montavont, A. (2008). Reading normal and

degraded words: Contribution of the dorsal and ventral visual pathways. NeuroImage, 40(1), 353- 366. doi:10.1016/j.neuroimage.2007.11.036. Retrieved; 06/06/2018.

[46] Lichtensteiger, J., Loenneker, T., Bucher, K., Martin, E., & Klaver, P. (2008). Role of dorsal and ventral stream development in biological motion perception. NeuroReport, 19(18), 1763-1767. doi:10.1097/wnr.0b013e328318ede3. Retrieved; 06/07/2018.

[47] Sherbondy, A. J., Dougherty, R. F., Napel, S., & Wandell, B. A. (2008). Identifying the human optic radiation using diffusion imaging and fiber tractography. Journal of Vision, 8(10), 12-12. doi:10.1167/8.10.12. Retrieved; 06/04/2018.

[48] Yogarajah, M., Focke, N. K., Bonelli, S., Cercignani, M., Acheson, J., Parker, G. J., . . . Duncan, J. S. (2009). Defining Meyers loop-temporal lobe resections, visual field deficits and diffusion tensor tractography. Brain, 132(6), 1656-1668. doi:10.1093/brain/awp114. Retrieved; 21/06/2018.

[49] Chen, C., Huang, F., Shao, H., Jin, J., Li, Z., & Zhang, C. (2009). Sectional Anatomy of the Optic Pathways on the Coronal Plane. Journal of the Chinese Medical Association, 72(10), 515-520. doi:10.1016/s1726-4901(09)70420-4. Retrieved; 05/07/2018.

[50] Zanon, M., Busan, P., Monti, F., Pizzolato, G., & Battaglini, P. P. (2009). Cortical Connections Between Dorsal and Ventral Visual Streams in Humans: Evidence by TMS/EEG Co-Registration. Brain Topography, 22(4), 307-317. doi:10.1007/s10548-009-0103-8. Retrieved; 27/05/2018.

[51] Bridgeman, B., A. H. C. Van Der Heijden, & Velichkovsky, B. M. (1994). A theory of visual stability across saccadic eye movements. Behavioral and Brain Sciences, 17(02), 247. doi:10.1017/s0140525x00034361. Retrieved; 22/06/2018.

[52] Fernandez-Miranda, J. C., Pathak, S., Engh, J., Jarbo, K., Verstynen, T., Yeh, F., . . . Friedlander, R. (2012). High-Definition Fiber Tractography of the Human Brain. Neurosurgery, 71(2), 430-453. doi:10.1227/neu.0b013e3182592faa. Retrieved; 18/06/2018.

[53] Wang, Q., Sporns, O., & Burkhalter, A. (2012). Network Analysis of Corticocortical Connections Reveals Ventral and Dorsal Processing Streams in Mouse Visual Cortex. Journal of Neuroscience,32(13), 4386-4399. doi:10.1523/jneurosci.6063-11.2012. Retrieved; 30/05/2018.

[54] Becker-Bense, S., Buchholz, H., Eulenburg, P. Z., Best, C., Bartenstein, P., Schreckenberger, M., & Dieterich, M. (2012). Ventral and dorsal streams processing visual motion perception (FDG-PET study). BMC Neuroscience, 13(1), 81. doi:10.1186/1471-2202-13-81. Retrieved; 24/05/2018.

[55] Vesia, M., & Crawford, J. D. (2012). Specialization of reach function in human posterior parietal cortex. Experimental Brain Research, 221(1), 1-18. doi:10.1007/s00221-012-3158-9. Retrieved; 02/06/2018.

[56] Filippi, C. G., & Cauley, K. A. (2012). Magnetic Resonance Diffusion Tensor Imaging and Diffusion
Tensor Tractography in the Evaluation of Congenital and Acquired Diseases of the Pediatric Visual System. Current Pediatric Reviews, 8(3), 232-236. doi:10.2174/157339612802139406. Retrieved; 21/06/2018.

[57] Tanaka, S., Moon, C., Fukuda, M., & Kim, S. (2011). Three-dimensional visual feature representation in the primary visual cortex. Neural Networks, 24(10), 1022-1035.doi:10.1016/j.neunet.2011.05.005. Retrieved; 16/06/2018.

[58] Dicarlo, J., Zoccolan, D., & Rust, N. (2012). How Does the Brain Solve Visual Object Recognition? Neuron, 73(3), 415-434. doi:10.1016/j.neuron.2012.01.010. Retrieved; 03/07/2018.

[59] Wu, W., Rigolo, L., O□donnell, L. J., Norton, I., Shriver, S., & Golby, A. J. (2012). Visual PathwayStudy Using In Vivo Diffusion Tensor Imaging Tractography to Complement Classic
Anatomy. Operative Neurosurgery, 70. doi:10.1227/neu.0b013e31822efcae. Retrieved; 01/07/2018.

[60] Cloutman, L. L. (2013). Interaction between dorsal and ventral processing streams: Where, when and how? Brain and Language, 127(2), 251-263. doi:10.1016/j.bandl.2012.08.003. Retrieved; 27/05/2018.

[61] Wärntges, S., & Michelson, G. (2014). Detailed Illustration of the Visual Field Representation along the Visual Pathway to the Primary Visual Cortex: A Graphical Summary. Ophthalmic Research,51(1), 37-41. doi:10.1159/000355464. Retrieved; 06/07/2018.

[62] Ackman, J. B., & Crair, M. C. (2014). Role of emergent neural activity in visual map development. Current Opinion in Neurobiology, 24, 166-175. doi:10.1016/j.conb.2013.11.011. Retrieved; 10/05/2018.

[63] Gervai, P. D., Sboto-Frankenstein, U. N., Bolster, R. B., Thind, S., Gruwel, M. L., Smith, S. D., & Tomanek, B. (2014). Tractography of Meyers Loop asymmetries. Epilepsy Research, 108(5), 872-882. doi:10.1016/j.eplepsyres.2014.03.006. Retrieved; 26/06/2018.

[64] Kamali, A., Hasan, K. M., Adapa, P., Razmandi, A., Keser, Z., Lincoln, J., & Kramer, L. A. (2014). Distinguishing and quantification of the human visual pathways using high-spatial-resolution diffusion tensor tractography. Magnetic Resonance Imaging, 32(7), 796-803. doi:10.1016/j.mri.2014.04.002. Retrieved; 12/05/2018.

[65] Hana, A., Husch, A., Gunness, V. R., Berthold, C., Hana, A., Dooms, G., . . . Hertel, F. (2014). DTI of the Visual Pathway - White Matter Tracts and Cerebral Lesions. Journal of Visualized Experiments,(90). doi:10.3791/51946. Retrieved; 06/07/2018.

[66] Thomas, C., Ye, F. Q., Irfanoglu, M. O., Modi, P., Saleem, K. S., Leopold, D. A., & Pierpaoli, C. (2014). Anatomical accuracy of brain connections derived from diffusion MRI tractography is inherently limited. Proceedings of the National Academy of Sciences, 111(46), 16574-16579. doi:10.1073/pnas.1405672111. Retrieved; 22/06/2018.

[67] Gilaie-Dotan, S. (2014). Ventral "form" visual pathway and the EBA are not critical for biological motion perception: Evidence from patients and a model suggestion. Journal of Vision, 14(10), 1327- 1327. doi:10.1167/14.10.1327. Retrieved; 09/06/2018.

[68] Lim, J. C., Phal, P. M., Desmond, P. M., Nichols, A. D., Kokkinos, C., Danesh-Meyer, H. V., . . . Moffat, B. A. (2015). Probabilistic MRI Tractography of the Optic Radiation Using Constrained Spherical Deconvolution: A Feasibility Study. Plos One, 10(3). doi:10.1371/journal.pone.0118948. Retrieved; 21/05/2018.

[69] Takemura, H., Rokem, A., Winawer, J., Yeatman, J. D., Wandell, B. A., & Pestilli, F. (2015). A Major Human White Matter Pathway Between Dorsal and Ventral Visual Cortex. Cerebral Cortex, 26(5), 2205-2214. doi:10.1093/cercor/bhv064. Retrieved; 13/05/2018.

[70] Polanen, V. V., & Davare, M. (2015). Interactions between dorsal and ventral streams for controlling skilled grasp. Neuropsychologia, 79, 186-191. doi:10.1016/j.neuropsychologia.2015.07.010. Retrieved; 06/06/2018.

[71] Silson, E. H., Chan, A. W., Reynolds, R. C., Kravitz, D. J., & Baker, C. I. (2015). A Retinotopic Basis for the Division of High-Level Scene Processing between Lateral and Ventral Human Occipitotemporal Cortex. Journal of Neuroscience, 35(34), 11921-11935. doi:10.1523/jneurosci.0137-15.2015. Retrieved; 30/07/2018.

[72] Kamali, A., Hasan, K. M., Adapa, P., Razmandi, A., Keser, Z., Lincoln, J., & Kramer, L. A. (2014). Distinguishing and quantification of the human visual pathways using high-spatial-resolution diffusion tensor tractography. Magnetic Resonance Imaging, 32(7), 796- 803. doi:10.1016/j.mri.2014.04.002. Retrieved; 15/05/2018.

[73] Foley, R. T., Whitwell, R. L., & Goodale, M. A. (2015). The two-visual-systems hypothesis and the perspectival features of visual experience. Consciousness and Cognition, 35, 225-233. doi:10.1016/j.concog.2015.03.005. Retrieved; 24/06/2018.

[74] Fang, F., & He, S. (2010). Cortical responses to invisible objects in human dorsal and ventral pathways. Journal of Vision, 5(8), 15-15. doi:10.1167/5.8.15. Retrieved; 11/07/2018.

[75] Azadbakht, H., Parkes, L. M., Haroon, H. A., Augath, M., Logothetis, N. K., Crespigny, A. D., . . .Parker, G. J. (2015). Validation of High-Resolution Tractography AgainstIn VivoTracing in the Macaque Visual Cortex. Cerebral Cortex, 25(11), 4299-4309. doi:10.1093/cercor/bhu326. Retrieved; 04/07/2018.

[76] Merabet, L. B., Devaney, K. J., Bauer, C. M., Panja, A., Heidary, G., & Somers, D. C. (2016). Characterizing Visual Field Deficits in Cerebral/Cortical Visual Impairment (CVI) Using Combined Diffusion Based Imaging and Functional Retinotopic Mapping: A Case Study. Frontiers in Systems Neuroscience, 10. doi:10.3389/fnsys.2016.00013. Retrieved; 01/06/2018.

[77] Pelekanos, V., Mur, M., & Storrs, K. R. (2016). Extracting Object Identity: Ventral or Dorsal Visual Stream? The Journal of Neuroscience, 36(24), 6368-6370. doi:10.1523/jneurosci.1102-16.2016. Retrieved; 26/06/2018.

[78] Gilaie-Dotan, S. (2016). Visual motion serves but is not under the purview of the dorsal pathway. Neuropsychologia, 89, 378-392. doi:10.1016/j.neuropsychologia.2016.07.018. Retrieved; 23/05/2018.

[79] Grigorian, A., Mcketton, L., & Schneider, K. A. (2016). Measuring Connectivity in the Primary Visual Pathway in Human Albinism Using Diffusion Tensor Imaging and Tractography. Journal of Visualized Experiments, (114). doi:10.3791/53759. Retrieved; 19/05/2018.

[80] Hajiabadi, M., Samii, M., & Fahlbusch, R. (2016). A preliminary study of the clinical application of optic pathway diffusion tensor tractography in suprasellar tumor surgery: Preoperative, intraoperative, and postoperative assessment. Journal of Neurosurgery, 125(3), 759-765. doi:10.3171/2015.6.jns1546. Retrieved; 22/06/2018.

[81] Aguirre, G. K., Datta, R., Benson, N., Prasad, S., Jacobson, S. G., Cideciyan, A. V., . . . Gennatas, E. (2016). Patterns of individual variation in visual pathway structure and function in the sighted and blind. doi:10.1101/065441. Retrieved; 09/07/2018.

[82] Sheth, B. R., & Young, R. (2016). Two Visual Pathways in Primates Based on Sampling of Space: Exploitation and Exploration of Visual Information. Frontiers in Integrative Neuroscience, 10. doi:10.3389/fnint.2016.00037. Retrieved; 27/04/2018.

[83] Rokem, A., Takemura, H., Bock, A. S., Scherf, K. S., Behrmann, M., Wandell, B. A., . . . Pestilli, F.
(2017). The visual white matter: The application of diffusion MRI and fiber tractography to vision science. Journal of Vision, 17(2), 4. doi:10.1167/17.2.4. Retrieved; 17/05/2018.

[84] Essayed, W. I., Zhang, F., Unadkat, P., Cosgrove, G. R., Golby, A. J., & Odonnell, L. J. (2017). White matter tractography for neurosurgical planning: A topography-based review of the current state of the art. NeuroImage: Clinical, 15, 659-672. doi:10.1016/j.nicl.2017.06.011. Retrieved; 11/06/2018.

[85] Simic, N., & Rovet, J. (2016). Dorsal and ventral visual streams: Typical and atypical development. Child Neuropsychology, 23(6), 678-691. doi:10.1080/09297049.2016.1186616. Retrieved; 12/05/2018.

[86] Agarwal, V., Malcolm, J. G., Pradilla, G., & Barrow, D. L. (2017). Tractography for Optic Radiation Preservation in Transcortical Approaches to Intracerebral Lesions. Cureus. doi:10.7759/cureus.1722. Retrieved; 07/07/2018.

[87] Freud, E., Culham, J., Plaut, D., & Behrmann, M. (2017). The large-scale organization of object processing in the ventral and dorsal pathways. Journal of Vision, 17(10), 286. doi:10.1167/17.10.286. Retrieved; 22/06/2018.

[88] Hales, P. W., Smith, V., Dhanoa-Hayre, D., Ohare, P., Mankad, K., Darco, F., . . . Clark, C. (2018). Delineation of the visual pathway in paediatric optic pathway glioma patients using probabilistic tractography, and correlations with visual acuity. NeuroImage: Clinical, 17, 541-548. doi:10.1016/j.nicl.2017.10.010. Retrieved; 17/05/2018.

[89] Zhan, M., Goebel, R., & Gelder, B. D. (2018). Ventral and Dorsal Pathways Relate Differently to Visual Awareness of Body Postures under Continuous Flash Suppression. Eneuro, 5(1). doi:10.1523/eneuro.0285-17.2017. Retrieved; 16/06/2018.